Strong Coupling Electroweak Symmetry Breaking*

Timothy L. Barklow
Stanford Linear Accelerator Center, Stanford University, Stanford CA 94309
Gustavo Burdman
Department of Physics, University of Wisconsin, Madison, WI 53706
R. Sekhar Chivukula and Bogdan A. Dobrescu
Department of Physics, Boston University, Boston, MA 02215
Persis S. Drell
Laboratory of Nuclear Studies, Cornell University, Ithaca, NY 14853-5001
Nicholas Hadley
Department of Physics, University of Maryland, College Park, MD 20742
William B. Kilgore
Fermi National Accelerator Laboratory, Batavia, IL 60510
Michael E. Peskin
Stanford Linear Accelerator Center, Stanford University, Stanford CA 94309
John Terning
Department of Physics, University of California, Berkeley, CA 94720
Darien R. Wood
Department of Physics, Northeastern University, Boston, MA 02115

ABSTRACT

We review models of electroweak symmetry breaking due to new strong interactions at the TeV energy scale and discuss the prospects for their experimental tests. We emphasize the direct observation of the new interactions through high-energy scattering of vector bosons. We also discuss indirect probes of the new interactions and exotic particles predicted by specific theoretical models.

I. INTRODUCTION

Though it is often said that the experiments of the last six years at LEP, SLC, and the Tevatron have brought no surprises, this very fact has led us into a new era in our understanding of particle physics. In the past, it has been possible to regard the $SU(2) \times U(1)$ gauge theory of the weak and electromagnetic interactions as a provisional theory, perhaps to be replaced by a model in which W bosons have constituents or internal structure. But the new experiments on the detailed properties of the Z and W bosons have confirmed the gauge theory predictions at the level of loop corrections. A striking aspect of this confirmation is the agreement between the value of the top quark needed to give the proper radiative corrections and the value of the top quark mass actually observed by the Tevatron collider experiments. The data compel us to accept $SU(2) \times U(1)$ as a fundamental gauge symmetry of Nature, a symmetry on the same footing as the gauge symmetry of electromagnetism.

At the same time, our increased understanding of the theory of electroweak interactions highlights the one central unsolved problem of that theory. In order that the W and Z bosons acquire mass, the $SU(2) \times U(1)$ gauge symmetry must be spontaneously broken. What *causes* this spontaneous symmetry breaking? At the moment, we have almost no experimental clue that bears on this question. In principle, the symmetry breaking may be caused by an elementary scalar field (the Higgs field) obtaining a vacuum expectation value, or by the vacuum expectation value of a composite operator. At this moment, it is more fashionable to assume that the symmetry breaking is caused by an elementary scalar field with only weak-coupling interactions. This viewpoint connects naturally to supersymmetry, which Marciano, in his introductory lecture at this meeting [1], called 'the only good idea out there'. On the other hand, it is attractive intuitively that an important rearrangement of symmetry such as we know occurs at the electroweak scale should result from new strong interactions. In this article, we will take this as our fixed idea and review its consequences in detail.

What, then, are the consequences of new strong interactions responsible for electroweak symmetry breaking? How will we investigate these new interactions experimentally? In particular, how much will we learn about them at the next generation of colliders?

Our discussion of these issues will proceed as follows: In Section II, we will review the present, rather weak, constraints on the nature of these new interactions. Sections III–VI, the heart of this review, will discuss direct experimental probes of the

* This work was supported in part by the U. S. Department of Energy and by the National Science Foundation.

new sector. These necessarily are experiments at very high energy, requiring also very high luminosity. In this sense, they test the ultimate reach of the colliders we are planning for the next generation, and for the more distant future. In Section III, we will present a general phenomenological theory of new strong interactions at the TeV scale, and we will raise a definite set of questions for experiment to address. In Section IV, we will review proposed experiments on the scattering of weak vector bosons through the new strong interactions. In Section V, we will discuss an experimental probe of the top quark's connection to the new interactions. In Section VI, we will summarize the sensitivity of these experiments to the resonances of the new strong interactions, and the complementarity of different experimental probes.

In Sections VII-IX, we will discuss additional consequences of the new strong interactions which are potentially accessible to experiments at lower energies. In Section VII, we will discuss possible anomalous gauge boson couplings and the manner in which these probe new strong interactions. In Section VIII, we review some more explicit models of strong-coupling electroweak symmetry breaking and explain how their specific dynamical assumptions lead to the prediction of exotic particles and interactions. In Section IX, we review experiments at present and future colliders which can search for the new particles predicted in these models.

Finally, in Section X, we summarize our discussion and present our general conclusions.

The reader experienced in the study of strong-coupling electroweak symmetry breaking will find relatively little new material in this review. Nevertheless, we feel that our time at Snowmass has been well spent. The members of our working group arrived at Snowmass with different types of expertise and very different preconceptions. We have appreciated the opportunity to discuss our areas of disagreement and to note how our ideas can fit together into a coherent overall picture. We hope that our improved understanding of this subject will be reflected here both in a clearer presentation of the main aims and directions of the study of new strong interactions and in a clearer understanding of the strengths and weaknesses of the experimental tools we hope eventually to bring to this problem.

II. EXPERIMENTAL CONSTRAINTS ON NEW STRONG INTERACTIONS

In this section, we discuss the present experimental constraints on new strong interactions responsible for electroweak symmetry breaking, and an important additional constraint that will come from future experiments.

A. Present Constraints

We begin with the information on the new strong sector that we have today. This will be a very short section. On the other hand, it is important to realize that some definite constraints are available. In particular, we know:

1.) The new strong interaction sector has an $SU(2) \times U(1)$ global symmetry, which it breaks spontaneously to $U(1)$.

That much is required just to couple it to the standard model gauge fields.

2.) The new strong interaction sector has an $SU(2)$ global symmetry which is not spontaneously broken.

The argument for this is that the relation

$$m_W/m_Z = \cos\theta_w \tag{1}$$

is satisfied to high accuracy; the violation of this relation, at a level below 1% depending on the definition of $\sin^2\theta_w$, is fully accounted for by the standard electroweak radiative corrections. At the same time, the photon mass is zero. To insure these two relations, the gauge boson mass matrix, in the $SU(2) \times U(1)$ basis (A^1, A^2, A^3, B), must have the form

$$m^2 = \frac{v^2}{4}\begin{pmatrix} g^2 & & & \\ & g^2 & & \\ & & g^2 & -gg' \\ & & -gg' & (g')^2 \end{pmatrix} . \tag{2}$$

Notice that the block of this matrix acting on the three $SU(2)$ gauge bosons is completely symmetric. If this mass matrix originates from a strong-coupling theory, this symmetry must reflect a property of that theory. The simplest possibility is an *unbroken* $SU(2)$ gauge symmetry under which the three $SU(2)$ currents transform as an isospin triplet [2, 3]. This symmetry is known as 'custodial $SU(2)$' symmetry.

3.) The mass scale of the new strong interaction sector is given by $v = 246$ GeV.

The value of v follows from the known values of the W and Z masses and the electroweak coupling constants, which are related by (2). The relation between v and the positions of strong-interaction resonances needs some extra discussion, which we will supply below.

4.) The new strong interactions are not just a scaled-up version of QCD.

This conclusion follows from a more detailed examination of the precision electroweak data. These measurements are often analyzed for the effects of new physics by introducing parameters S, T, U which represent the effects of new particles on the Z and W vacuum polarization diagrams [4]. In particular, S, a finite part of the Z field strength renormalization, can be predicted in quite a clean way if one assumes that the new interactions resemble scaled-up QCD. The result is $S = 0.3 \pm 0.1$. This should be compared to the value for S which is obtained by fitting the deviation of the electroweak data from the standard model predictions for a Higgs boson mass of 1 TeV [5]:

$$S = -0.26 \pm 0.16 . \tag{3}$$

The results are inconsistent at the 3 σ level. We will discuss the properties of models which ameliorate this problem in Section VII.

B. No Light Higgs?

There is a fifth piece of information which is not yet available but which will have an important influence on this experimental program when it does become known. This is the question of whether there is a light Higgs particle. We will emphasize in this report that the experiments which will explore the structure of the new strong interactions are difficult ones, requiring high luminosity and high energy. Thus it will be important to know in advance whether one really needs this strong-interaction hypothesis to explain electroweak symmetry breaking. That question can be addressed experimentally.

The alternative to electroweak symmetry breaking through new strong interactions is the possibility of electroweak symmetry breaking due to the vacuum expectation values of one or more light scalar fields. We can rule out this alternative if these scalar fields are not discovered in collider experiments. These issues are discussed in more detail in the working group report on weakly coupled Higgs bosons [6].

First of all, we should ask whether there exist light scalar particles, detectable, for example, through their $b\overline{b}$ or $\gamma\gamma$ decay modes. The experiments which search for these particles have been given a prominent role in discussions of all future colliders. It is likely that a light scalar, if it exists, will be discovered at the LHC if not before. However, the simple existence of these particles is not sufficient information, because there are several ways to obtain particles of this sort, as bound states of more elementary constituents, in models in which $SU(2) \times U(1)$ breaking arises from new strong interactions. We will discuss several examples in Section VIII. Because of this, it is also important to determine whether a light scalar particle which has been observed plays a direct role in electroweak symmetry breaking.

This can be done by observing the coupling of the scalar to ZZ or WW. If we write an $SU(2) \times U(1)$ invariant effective Lagrangian, with several neutral scalar particles ϕ_i assigned (for simplicity) a common weak isospin I^3, the coupling of these scalars to WW and ZZ is given by

$$\Delta\mathcal{L} = (2I^3)^2 \sum_i \frac{w_i}{v^2} \left(m_Z^2 Z_\mu Z^\mu + 2m_W^2 W_\mu^+ W^{-\mu} \right) \phi_i \ , \quad (4)$$

where

$$w_i = \sqrt{2}\, \langle \phi_i \rangle \ . \quad (5)$$

and v is the scale given in item 3 above. If

$$\sum_i (2I^3)^2 w_i^2 = v^2 \ , \quad (6)$$

then the vacuum expectation values of the fields ϕ_i are completely responsible for the generation of the Z and W masses through the breaking of $SU(2) \times U(1)$. If particles are not found which saturate the sum rule (6), then the mechanism of $SU(2) \times U(1)$ breaking necessarily acts at higher energies. Because a Higgs particle can be heavy only if it is strongly self-coupled, this mechanism would also necessarily involve new strong interactions.

It is difficult to measure the vacuum expectation values w_i at hadron colliders. This coupling is best observed in the process $q\overline{q} \to W\phi$, with ϕ decay to $b\overline{b}$. For standard model coupling ($w = 1$), this process can be observed at the upgraded Tevatron up to a ϕ mass of about 110 GeV, depending on the final integrated luminosity [7], and over roughly the same range at the LHC [8]. At electron colliders, where the dominant process for Higgs boson production is $e^+e^- \to Z^0\phi$, this experiment is quite straightforward. In particular, once the mass of the ϕ is given, the measurement of w involves only counting Z^0 bosons produced at a fixed lab energy and can be done without assumptions on the ϕ decay scheme [9]. If the bosons are found which saturate the sum rule (6), these particles hold the physics of electroweak symmetry breaking. If they are not found, we will know that we need the experimental program for very high energies that we will set out below.

We should note that it is possible that a light Higgs boson responsible for electroweak symmetry breaking could also be a composite bound by new strong interactions. Models of this type were introduced many years ago by Kaplan and Georgi [10] and have also appeared recently in the context of supersymmetry model-building [11]. In this case, the scale of new strong interactions can lie at a multi-TeV mass scale. We will not discuss these models further in this report.

III. NEW PION DYNAMICS

Although we do not know much about the nature of the new strong interactions, we know enough to suggest a general route for experimental analysis. In this section, we will set out a general phenomenology of the new strong interactions which can provide a guide for us in the discussion of experiments.

From items 1 and 2 above, we know that the new strong interactions contain the pattern of spontaneous global symmetry breaking:

$$SU(2) \times SU(2) \to SU(2) \ , \quad (7)$$

which is identical to the symmetry breaking pattern of QCD in the limit of zero mass for the u and d quarks. From here on, to promote this analogy, we will refer to this zero quark mass limit of QCD simply as 'QCD', and we will refer to the unbroken $SU(2)$ symmetry of the new strong interactions as 'isospin'. Then, for both the familiar and the new theory of strong interactions, Goldstone's theorem implies that there should exist an isospin triplet of massless mesons, the pions (π^+, π^-, π^0). Further, the fact that these particles are Goldstone bosons resulting from spontaneous symmetry breaking leads to a systematic set of predictions for the low-energy behavior of their interactions, predictions which are in fact valid experimentally after a correction is made for the effects of the nonzero quark masses.

In the familiar strong interactions, the formalism which gives these predictions is known as 'current algebra'. Where current algebra predicts a property of the familiar pions, the same property must hold for the pions of the new strong interactions. However, outside the domain controlled by current algebra, the properties of these new pions could be completely different from the QCD expectation. How the new pions behave at high energy, we must find out experimentally.

The idea that the new strong interactions, just like QCD, have pions as their lightest states gives focus to the experimental pro-

gram to investigate these new interactions. It suggests that we approach the study of these new interactions by asking the same questions that we asked in the 1950's about low-energy QCD. Of course, we should be prepared that the *answers* to these questions may be completely different.

A. Who are the Pions?

First of all, we must clarify where the new pions can be found. How do we create a beam of the new pions, or look for them in the final state of a high-energy reaction?

In the new strong interactions, the spontaneously broken $SU(2)$ is coupled to the gauge bosons of the standard model. When the symmetry breaks, the weak gauge bosons obtain mass. Since a massless gauge boson has two transverse polarization states, but a massive spin-1 boson has three polarization states, each of these bosons must acquire an additional degree of freedom. It is well known that they do this by absorbing the corresponding Goldstone boson resulting from the global symmetry breaking. This is the essence of the Higgs mechanism.

This statement of the Higgs mechanism has an interesting converse. When a massive spin-1 boson is boosted to high energy, it again has well-defined transverse and longitudinal polarization states. The transverse polarization states have couplings which approach those of the original massless bosons. The interactions of the longitudinal polarization states of the spin-1 boson become equal to those of the Goldstone boson that it ate to become massive. This result is known as the 'Goldstone boson equivalence theorem' [12, 13, 14]; see Figure 1.

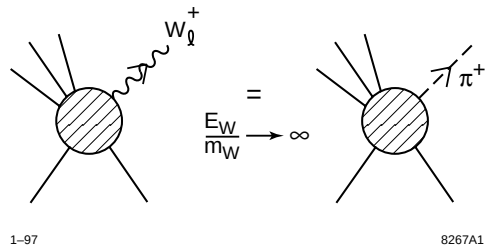

Figure 1: The Goldstone Boson Equivalence Theorem.

The Goldstone boson equivalence theorem implies that the longitudinal polarization states of W and Z play the role of the pions in the new strong interactions. Any collider process which involves W and Z bosons in the initial or final state can in principle give us access to these new interactions. In the next several sections, we will discuss the most important reactions for the future study of these new pion processes.

To complete the connection between W and Z dynamics and the dynamics of new pions, we can add one more piece of information. It is possible to derive the W and Z mass matrix predicted by the new strong interaction theory by analyzing matrix elements of the $SU(2) \times U(1)$ gauge currents. Assuming the symmetry-breaking pattern (7), we must obtain a mass matrix of the form (2). But this derivation also identifies the overall scale v in (2) as being equal to the pion decay constant:

$$f_\pi = v = 246 \text{ GeV} . \tag{8}$$

Through this relation, we can convert the known masses of the W and Z to the mass scale of the new strong interactions.

B. Pion-Pion Scattering

The most basic question that we could ask about the new strong interactions is: What is the nature and strength of the low-lying resonances? The analogy to pion dynamics in QCD tells us that we should think especially about resonances that couple to two-pion scattering channels. From the scale given by (8), we should expect these 'low-lying' resonances to be found at TeV energies.

In pion-pion scattering, Bose statistics dictates the principal scattering channels at low energy. These have total spin J and isospin I given by:

$$\begin{aligned} J = 0 \qquad & I = 0, 2 \\ J = 1 \qquad & I = 1 . \end{aligned} \tag{9}$$

From now on, we will refer to these three channels by the value of I. We will discuss in a moment how to look for resonances in these channels using longitudinal W and Z bosons as our tools.

Current algebra predicts the leading behavior of the pion-pion scattering amplitude near threshold. Specifically, it predicts

$$a_I = \frac{s}{A_I} + \mathcal{O}(s^2) \tag{10}$$

where A_I, the relativistic generalization of the scattering length, is given in the three relevant channels by

$$\begin{aligned} A_0 &= 16\pi f_\pi^2 = (1.7 \text{ TeV})^2 \\ A_1 &= 96\pi f_\pi^2 = (4.3 \text{ TeV})^2 \\ A_2 &= -32\pi f_\pi^2 . \end{aligned} \tag{11}$$

The channels I=0 and 1 are attractive at low energy, and so one might expect to see resonances here. In fact, a more powerful statement is possible. Unitarity implies that $\text{Im}(a_I) = |a_I|^2$, which implies that $\text{Re}(a_I) < 1/2$. The corrections to (10) must become important and restore $a_I(s)$ to an expression consistent with unitarity before this criterion is met [13], that is, for

$$I = 0 : \ \sqrt{s} < 1.3 \text{ TeV} , \quad I = 1 : \ \sqrt{s} < 3.0 \text{ TeV} . \tag{12}$$

If unitarity is restored through resonances, as it is in the familiar strong interaction, we would expect the first resonance in each channel to appear below these limits. For comparison, the most prominent low-energy resonance in QCD is the ρ. Scaling up m_ρ by the ratio of f_π's, we find

$$m_\rho^{\text{new}} = \frac{f_\pi^{\text{new}}}{f_\pi^{\text{old}}} m_\rho^{\text{old}} = \frac{246 \text{ GeV}}{93 \text{ MeV}} m_\rho = 2 \text{ TeV} \tag{13}$$

as an alternative estimate of the I=1 resonance mass.

In the literature, a prominent I=J=1 resonance in the new strong interactions is called a 'technirho'. By analogy, a prominent I=0, J=1 resonance is called a 'techniomega'. As in QCD,

the techniomega will not couple to $\pi\pi$, but it may appear in e^+e^- and $q\overline{q}$ annihilation, decaying to 3π or $\gamma\pi$ final states. Through the latter channel, the techniomega can appear as a resonance in γZ^0. While the technirho, if it exists, must couple to a virtual γ or Z^0, for the techniomega this is a model-dependent question.

When we compute the sensitivity of collider experiments to resonances of the new strong interactions, and we consider parton-level processes which extend above 1 TeV in center-of-mass energy, we must be careful to respect unitarity. A direct, if simple-minded, way to do this is to parametrize the *phase shift* in each of the three relevant channels by the expression

$$\tan\delta_I = \frac{s}{A_I}\frac{1}{1-s/M_I^2}\,. \qquad (14)$$

This expression automatically respects unitarity and the predictions of current algebra. It includes a resonance at the mass M_I. It has a sensible limit $M_I \to \infty$ which is determined only by current algebra and unitarity. In the literature, the limit of a unitarized but nonresonant pion-pion scattering amplitude is known as the 'low energy theorem' (LET) model. The precise definition of the LET limit depends on the unitarization procedure and thus varies somewhat from author to author. All of these prescriptions give similar results for $\pi\pi$ center-of-mass energies in the region (12).

The simple parametrization (14) does not take account of crossing relations which connect the amplitudes in the three channels (and additional channels which become important at higher energies). The detailed calculations of the signatures of pion-pion scattering processes in high-energy colliders [15, 16] have used somewhat more sophisticated but less transparent parametrizations. A different strategy has been to apply the low-energy expansion of the effective Lagrangian for pion-pion scattering, studied by Gasser and Leutwyler [17]. This approach does not give manifestly unitary scattering amplitudes, but it does give the correct crossing relations. In particular, the three coefficients of order s^2 in the formulae for the $a_I(s)$ are given in terms of two constants L_1, L_2. Pion-pion scattering processes of new strong interactions have been studied in this parametrization in [18, 19, 20, 21].

C. Strategies for Pion-Pion Scattering Experiments

There are two strategies for measuring the pion-pion scattering amplitudes at colliders. These are illustrated in Figure 2. In the first of the processes shown, longitudinally polarized W bosons are radiated from incident fermions, and these scatter to vector boson pairs at large transverse momentum. In the second process, the incident fermions annihilate directly to vector boson pairs, which show the effects of new strong interactions through the production form factor. The incident fermions could be either quarks or leptons. In either case, the subprocess energy must be of order 1 TeV to see significant effects.

We will now make some general comments which provide theoretical orientation on these two processes. In Section IV, we will discuss simulation studies of these two reactions and see what sensitivity they can achieve in realistic settings.

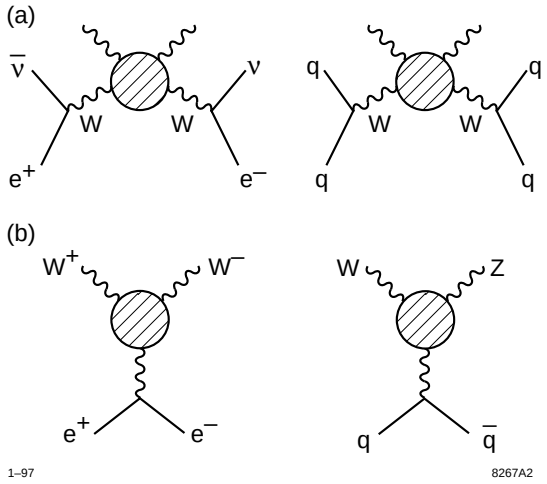

Figure 2: Processes which measure the pion-pion scattering amplitudes of new strong interactions.

The vector boson scattering process illustrated in Figure 2(a) can in principle access all three of the dominant channels of pion-pion scattering. The channels are distinguished by the identity of the final vector bosons: W^+W^+ or W^-W^- couples only to I=2, W^+Z^0 to I=1,2, and Z^0Z^0 to I=0,2. The cross sections must be summed over the vector bosons which appear in the initial state, though typically they are dominated by channels with initial W's. This is especially true in e^+e^- reactions, since the probability for an electron to radiate a Z is about 1/10 of the probability to radiate a W. In pp reactions, all of these processes occur in the same environment; at an e^+e^- machine, experiments on the I=2 channel require dedicated operation of the accelerator as an e^-e^- collider.

The production of transversely polarized W pairs is not influenced significantly by the new strong interactions and so should be treated as a background. Often in the literature, the signal of new strong interactions is expressed as the difference between the high-p_T vector boson yield in the strong interaction model and the yield in the minimal standard model with a Higgs boson of mass about 100 GeV. The latter assumption turns off the new strong interactions but retains the production of transversely polarized boson pairs through standard model gauge interactions.

Additional backgrounds come from processes of different topology that lead to vector boson pairs or from final states that fake vector boson pairs. At the LHC, an important background reaction is the ubiquitous $gg \to gg$, with the final jets broadened to the W mass. To overcome this problem, it is typically required that vector bosons are observed in their leptonic decay modes. Even with this requirement, processes such as $gg \to t\overline{t}$ and $gq \to Wq$ must be removed carefully with targeted cuts. At high energy e^+e^- colliders, the most important backgrounds come from photon-induced processes such as $\gamma\gamma \to W^+W^-$ and $\gamma e \to WZ\nu$. These are removed by a forward electron

veto and by requiring that the vector boson pair has a transverse momentum of order m_W. The kinematic requirements of these cuts, and consideration of the overall rate, call for observation of the W and Z in their hadronic decay modes.

In very favorable circumstances, a resonance of the new strong interactions can produce a peak in the mass spectrum of vector boson pairs. However, the more typical situation is that it produces only a shoulder or an enhancement over the prediction of a weak-coupling model. It is therefore a crucial experimental problem to understand the standard model sources of vector boson pairs and other sources of background *quantitatively*, so that these effects can be subtracted accurately.

The fermion annihilation process illustrated in Figure 2(b) is restricted to angular momentum J=1, and therefore to the I=1 channel of pion-pion scattering. We should note, though, that in QCD this channel contains the ρ meson and thus has the strongest resonant effects at low energy.

We can parametrize the strong interaction effects on vector boson pair production by a form factor $F_\pi(q^2)$, the pion form factor of the new strong interactions. The amplitude for e^+e^- or $q\overline{q}$ annihilation to new pions or longitudinally polarized W and Z pairs is enhanced by the factor $F_\pi(s)$. The form factor satisfies $F_\pi(0) = 1$ and should show an enhancement at the mass of any I=1 resonance. If there is a strong I=1 resonance, the form of the function will be described by a vector meson dominance parametrization

$$F_\pi(s) = \frac{-M_1^2 + i\Gamma M_1}{s - M_1^2 + i\Gamma M_1}. \qquad (15)$$

There is an additional piece of information about F_π which is known more rigorously. Assuming only that $\pi\pi \to 4\pi$ processes are unimportant at a given energy, the *phase* of $F_\pi(s)$ is precisely the I=1 $\pi\pi$ phase shift $\delta_1(s)$. Thus, even in a nonresonant model, it is possible to detect the presence of new strong interactions if one can measure the imaginary part of $F_\pi(s)$.

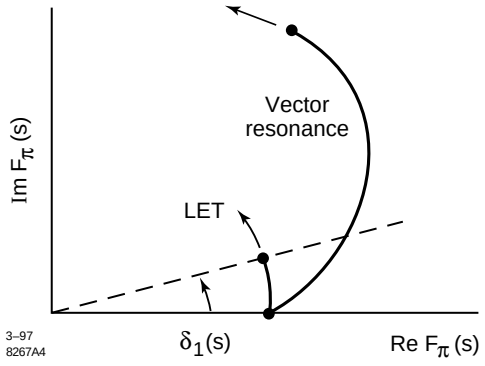

Figure 3: Dependence of $F_\pi(q^2)$ on energy, in models without and with a new strong interaction resonance in the I=J=1 channel.

In Figure 3, we show how the amplitude $F_\pi(s)$ moves in the complex plane as s increases, for the case of a nonresonant model with phase shift $\delta_1(s)$. We also show the motion of $F_\pi(s)$ for a resonant model in which, when the resonance is reached, the phase shift goes through $\pi/2$.

At the LHC, the main effect of the new pion form factor is to create strong-interaction resonances in $q\overline{q}$ annihilation. These can show up as peaks in the WZ mass distribution if the resonance mass is sufficiently low. In high-energy e^+e^- colliders, which are designed to measure the differential cross section for $e^+e^- \to W^+W^-$ to percent accuracy, it is possible to measure the deviation of F_π from 1 below the resonance or in a nonresonant case. In particular, it is possible to measure the phase of F_π from the interference of longitudinal and transverse W pair production.

IV. EXPERIMENTAL PROSPECTS FOR THE STUDY OF NEW PION INTERACTIONS

In this section, we will review simulation studies from the literature and new studies that have been done at Snowmass that have explored the experimental reach of future experiments on the new pion interactions. These experiments are among the most difficult proposed for the next generation of accelerators. They require parton center-of-mass energies above 1 TeV and luminosities sufficient to observe hard scattering cross sections at these energies. Thus, they tax the highest energies and luminosities of future generations of colliders.

For this reason, we will concentrate our attention on the LHC at full design luminosity and a high-luminosity electron-positron linear collider with 1.5 TeV in the center-of-mass. Throughout this report, we will use the shorthand 'NLC' to refer to a next-generation e^+e^- collider.

The experimental studies that we will review in this section made a variety of assumptions on the collider luminosity. In this section, whenever we present the results of a simulation, we will give the size of the data sample assumed. When we assemble and interpret these results in Section VI, we will scale all results to data samples of 100 fb^{-1} (1 year at peak luminosity of 10^{34} cm^{-2}s^{-1}). In all cases, we assume the full energy reach of the machine (14 TeV for the LHC and 1.5 TeV for the NLC). In addition, we assume 80% electron polarization at the linear collider. These reference machine parameters are listed in Table I. At the end of Section VI, we will comment briefly on what can be learned from even higher energies and luminosities.

Table I: Reference machine parameters, energy, luminosity, and polarization, for studies of new pion scattering.

	CM Energy (TeV)	$\mathcal{L}$ (cm^{-2}s^{-1})	P
LHC	14	10^{34}	
NLC	1.5	10^{34}	$P_e = 80\%$

A. Analysis Methods

The strategies for studying these new strong interactions have been discussed in Section IIIC. The basic signals are (1) a peak in the mass spectrum of vector boson pair production which

is a straightforward signal to extract, (2) a broad enhancement in the cross section for boson boson scattering which involves an absolute cross section measurement and a detailed understanding of all backgrounds, and (3) a helicity analysis of $e^+e^- \to W^+W^-$ which allows the measurement of the I=1 phase shift in that channel.

Many studies exist that probe the reach of the LHC and the NLC to discover the new strong interactions. Most studies rely on parton level estimates for the signal and background processes. For the LHC, the most detailed studies are those of the detector collaborations ATLAS and CMS [8, 22, 23]. The backgrounds are large, and care has been taken to try to estimate the backgrounds realistically. Modern parton distribution functions tuned to Tevatron data are used. At high luminosity, the LHC experiments expect 25 minimum bias events per crossing. The effect of these events is included. Still, these analyses do not involve full detector simulations. Instead, GEANT simulations of the momentum resolution, radiation losses and isolation effects in the detectors are parametrized and then implemented with Gaussian smearing.

At the NLC, where backgrounds and detector resolutions are much less of a concern, most studies use reasonable parametrizations of detector efficiencies and resolution, but do not involve detector simulation. For the study of the reaction $e^+e^- \to W^+W^-$, four vectors of stable particles emerging from the reactions are smeared assuming Gaussian errors according to the parametrizations summarized in [9]. Studies of boson scattering processes such as $e^+e^- \to \nu\overline{\nu}WW$ or $e^+e^- \to \nu\overline{\nu}ZZ$ are somewhat more idealized.

The goals for the simulation studies are to determine (1) whether we can conclusively observe pion-pion scattering due to new strong interactions, and (2) what can be determined about the structure and resonances of the new strong interaction sector. In evaluating the results we will present below, it is important to realize that, by the time these experiments are done, the alternative explanation of electroweak symmetry breaking through the vacuum expectation values of light scalar fields will have been excluded at a high level of confidence. We have discussed this point in Section IIB.

B. Studies of New Strong Interactions at the LHC

At the LHC, the main difficulty for experiments probing strong symmetry breaking is backgrounds. In most studies, the two final state gauge bosons are reconstructed in their "gold plated" leptonic modes only, although some studies have been able to demonstrate significant signals in so called "silver plated" modes where one gauge boson decays leptonically and the other decays to 2 jets. Table II lists the detection modes and isospin channels accessible at the LHC. (In our notation, qq refers to a reaction of quarks with the same or with different flavors.) The analyses suffer from low statistics, in part because they select modes with small decay branching ratios, but the high transverse momentum, isolated leptons characteristic of the leptonic decay modes provide clean signatures for gauge bosons in the final state.

Table II: Detection modes and isospin channels accessible at the LHC.

Parton Level Process	Weak Isospin
$qq \to qqZZ$	0, 2
$qq \to qqW^+W^-$	0, 1, 2
$qq \to qqWZ$	1, 2
$qq \to qqW^\pm W^\pm$	2
$q\overline{q} \to ZZ$	0,2
$q\overline{q} \to Z\gamma$	0
$q\overline{q} \to ZW$	1

1. Resonance Searches

Both ATLAS and CMS have studied the ability of their experiments to discover resonances in diboson production due to new strong interactions. The ATLAS technical proposal [23] describes a search for evidence of a technirho (ρ_T) decaying to WZ or a techniomega (ω_T) decaying to $Z\gamma$.

In the I=1 channel, they estimate that, for a 1 TeV ρ_T, the signal production cross section is 40 fb. This comes from a combination of direct production ($qq \to WZ$) and boson-boson scattering ($qq \to qqWZ$), though the annihilation channel dominates. The experimental signature is three isolated, high transverse momentum leptons in the final state, together with significant missing energy. In the study, the missing transverse energy was computed after energy smearing, using the momentum vectors of all particles observable in the detector. A W mass constraint was then applied to the lepton-neutrino pair in order to reconstruct the total invariant mass of the WZ system.

The dominant background is $t\overline{t}$ production with one dilepton combination having a mass close to the Z mass. This background is effectively removed by the isolation cuts on the leptons and the W mass constraint described above. The other backgrounds are reactions that produce transversely polarized WZ pairs, continuum $q\overline{q} \to WZ$ and boson-boson scattering through $qq \to qqWZ$. Note that because the cross section is dominated by the annihilation channel, there is no advantage in tagging forward jets to select the boson-boson scattering reaction.

The reconstructed diboson mass for a 1 TeV ρ_T decaying to WZ, for 100 fb^{-1} of data at the LHC, is shown in Figure 4(a). The backgrounds remaining after all cuts are small and the resonance is sufficiently narrow that the signal would be straightforward to observe. This analysis can be extended to search for vector resonances at LHC up to a mass of 1.6 TeV with 100 fb^{-1} of data [23, 24].

The search for an ω_T resonance is quite similar. As we have noted in Section IIIB, the ω_T is not produced in boson-boson scattering; also, it is a model-dependent question whether it couples to $q\overline{q}$ annihilation. If it does couple, it can produce a dramatic effect, since the ω_T can decay to γZ^0, which is directly reconstructed if the Z decays leptonically. The dominant backgrounds are continuum $Z\gamma$ production and $Z+$ jet production where the jet fakes an isolated photon. The production cross section for a 1.46 TeV ω_T is expected to be approximately 50

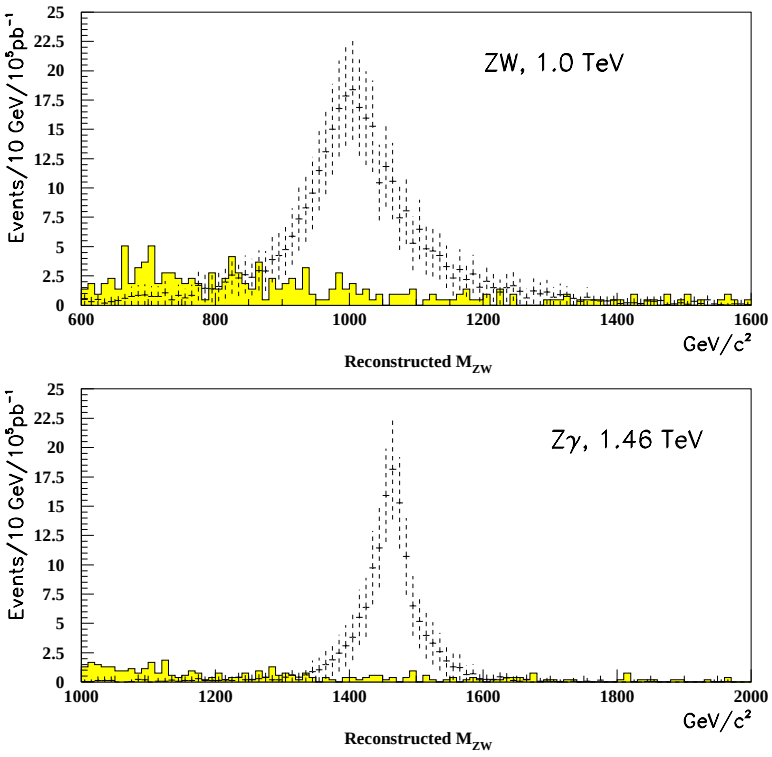

Figure 4: Reconstructed masses for high mass resonances decaying into gauge boson pairs, from [23]: (a) Signal of a 1 TeV ρ_T decaying to WZ and subsequently to three leptons (b) Signal of a 1.46 TeV ω_T decaying to $Z\gamma$ with the Z then decaying to two leptons.

fb. Figure 4(b) shows the reconstructed $Z\gamma$ mass distribution for the expected signal in a 100 fb^{-1} data set. This search is sensitive to ω_T up to approximately 2 TeV.

2. *Absolute Cross Section Measurements*

If the resonances in the new strongly coupled world are too massive or too broad, we will not be able to see them directly as peaks in a diboson mass spectrum. In that case, we can only look for the effects of the new interactions as event excesses or cross section enhancements in the various boson-boson scattering channels. The largest enhancements will appear in the isospin channel corresponding to the quantum numbers of the strongest resonance. At a certain point, however, our sensitivity to the mass of the object dominating the scattering channel will be lost. Then we may still be able to establish the existence of new strong interactions, but we will be unable to distinguish anything about their detailed structure.

At the LHC, the most sensitive channel for probing the high mass structure of the new strong interaction is $qq \rightarrow qqW^{\pm}W^{\pm}$. This channel minimizes the backgrounds from pair-production of transversely polarized W bosons, since the $W^{\pm}W^{\pm}$ final state cannot result from an annihilation process, and it minimizes the background from $t\bar{t}$ production leading to hard isolated leptons.

The experimental signal is the observation of two isolated same-sign leptons in the central detector, with large dilepton invariant mass. The dominant backgrounds come from electroweak bremsstrahlung processes, gluon exchange, $W+t\bar{t}$ production, WZ and ZZ final states, and $t\bar{t}$ production. In the ATLAS study of this decay mode, the dominant background processes from $t\bar{t}$, WZ and ZZ were generated using PYTHIA 5.7 and the other backgrounds were simulated at the parton level. Detector acceptance and resolution for leptons and jets were included in the simulation.

The signal could only be observed above background if the analyses made cuts on the distinctive topology of the boson scattering process. Signal events have two jets in the forward regions of the detector from the scattered quarks, but there is not much jet activity in the central detector if one has required both W bosons to decay leptonically. The $t\bar{t}$ background is greatly reduced by rejecting events with a jet of significant energy in the central detector, and all backgrounds not originating from boson fusion are reduced by requiring the tagging of two jets, one in each of the forward detector regions. The dominant background remaining after all cuts is transverse W pair production.

The event rates in this channel are low and the signal to background ratio does not change much as a function of lepton transverse energy. Figure 5 shows the signal expected for a model in which a 1 TeV I=J=0 particle (a massive Higgs scalar) is exchanged in the t-channel. The review [25] provides a com-

prehensive survey of this channel for a variety of hypotheses of the source of the strong symmetry breaking (scalar or vector resonances with a variety of masses). In all cases, there is no resonance shape to distinguish signal from background and the signal can only be extracted if the absolute magnitude of the background is known from other sources. However, if one does understand the backgrounds [26] and can accurately model the jet tagging and jet vetoing in the high luminosity environment of the LHC, studies show that the $qq \to qq' W^{\pm} W^{\pm}$ channel is sensitive to strong electroweak symmetry breaking even in the LET limit. No matter how high one places the masses of resonances, there will be a significant excess of events over background in this channel. In other words, this channel will discover the new strong interactions if they are there.

The yields in this channel, in the LET limit, for a 100 fb^{-1} data sample are listed in the general summary of the results of simulation studies which we present in Table IV of Section VI.

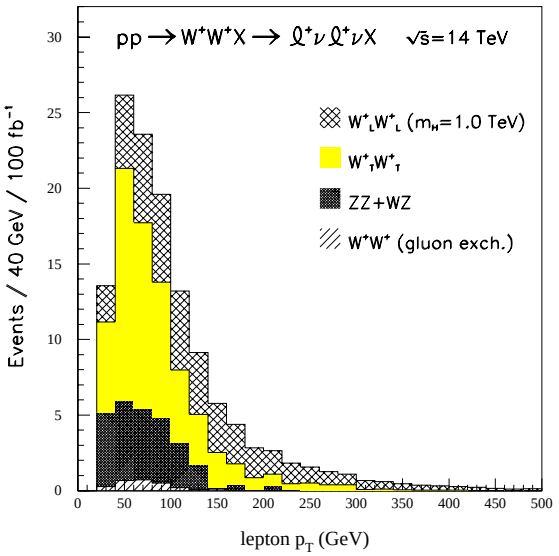

Figure 5: Expected numbers of $W^+W^+ \to (l\nu)(l\nu)$ signal and background events after all cuts for a 100 fb^{-1} data sample at the LHC, from [23]. The signal corresponds to a 1 TeV Higgs.

C. Studies of New Strong Interactions at the NLC

At the NLC, the available channels for studying strong symmetry breaking are limited by rate rather than backgrounds. The boson-boson scattering processes that can be studied are listed in Table III. All studies use the 2 jet decays of the gauge bosons to take advantage of the largest accessible branching ratios. The I=2 final state W^-W^- can also be studied at a linear collider; however, this requires a dedicated experiment of several years' duration with e^-e^- collisions. It is interesting that this information is potentially available, but we will not consider this process further here.

Another tool available at NLC is the annihilation channel $e^+e^- \to W^+W^-$. The rates are high enough and backgrounds low enough that one can do a helicity analysis by reconstructing the production and decay angles of the W's in the final state. This allows one to separate the longitudinal and transverse contributions to the final state, and to measure the new pion form factor discussed in Section IIIC.

Table III: Detection modes and isospin channels accessible at the NLC.

Parton Level Process	Weak Isospin
$e^+e^- \to \nu\overline{\nu}ZZ$	0, 2
$e^+e^- \to \nu\overline{\nu}W^+W^-$	0, 1, 2
$e^+e^- \to W^+W^-$	1

1. *Boson-Boson Scattering at the NLC*

A study of the boson scattering processes at an e^+e^- linear collider, $e^+e^- \to \nu\overline{\nu}WW$ and $e^+e^- \to \nu\overline{\nu}ZZ$ is described in [27] and reviewed in a contribution [28] to these proceedings. Here we will summarize only the essential features of the analysis. The gauge bosons are each reconstructed in the dijet final state. With realistic jet energy resolutions, the W and Z bosons cannot be discriminated on an event-by-event basis, but they can be separated statistically. The dominant backgrounds are dibosons produced from e^+e^- annihilation, $e^+e^- \to e^+e^-W^+W^-$, and $e^+e^- \to e\nu WZ$, with misidentification of WZ events as either WW or ZZ events due to jet energy smearing. The study [27] does not include detector resolution or efficiencies except in the important area of jet energy resolution where $\Delta E_j/E_j = 50\%/\sqrt{E_j} \oplus 2\%$ is assumed.

The annihilation background is removed by a cut requiring significant missing mass in the event. One first requires W^+W^- events to have large WW invariant mass and a large angle with respect to the beam axis ($|\cos\theta_W| < 0.8$). The dominant backgrounds then come from $e^+e^- \to e^+e^-W^+W^-$ and $e^+e^- \to e\nu WZ$, due to intermediate states with virtual photons radiated from the electron lines. These backgrounds are suppressed by the requirement that the transverse momentum of the WW system be large (50 GeV $< p_T(WW) <$ 300 GeV), and by a veto on events with hard forward electrons. For the veto, it is assumed that electrons with $E_e > 50$ GeV can be tagged for $|\cos\theta_e| < 0.99$ [9]. With this series of cuts, the strong symmetry breaking signals are observable over background.

The resulting WW and ZZ signals, for a 200 fb^{-1} data sample at a 1.5 TeV NLC, are shown in Figure 6 as a function of the diboson invariant mass. As was the case at the LHC, the signal to background ratio does not change significantly as a function of this mass, and there is no resonance shape to distinguish signal from background unless the resonance masses are very low (or order 1 TeV). Thus, again, the signal can only be extracted if the absolute magnitude of the background is known from other sources. However, if the background can be accurately modeled, the study of [27] shows that the $e^+e^- \to \nu\overline{\nu}ZZ$ channel is sensitive to strong electroweak symmetry breaking to the LET limit.

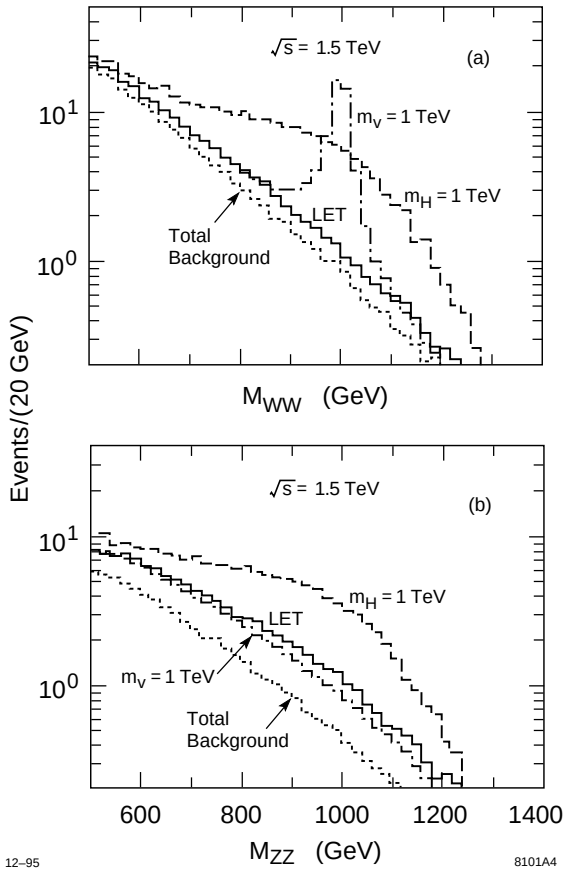

Figure 6: Expected numbers of $W^+W^-, ZZ \to (jj)(jj)$ signal and background events after all cuts for a 200 fb^{-1} unpolarized data sample at the NLC at 1.5 TeV, from [27]: (a) $e^+e^- \to \nu\overline{\nu}W^+W^-$, (b) $e^+e^- \to \nu\overline{\nu}ZZ$. The dotted histogram shows the total standard model background including misidentifications. The solid histogram shows signal plus background for the LET.

2. *Helicity Analysis of $e^+e^- \to W^+W^-$ at the NLC*

As was discussed in Section IIIC, the annihilation channel $e^+e^- \to W^+W^-$ can be used to probe the new strong interactions because final state rescattering provides information about the J=1 partial wave in the process $W_L^+W_L^- \to W_L^+W_L^-$. The strategy of the analysis is to use the decay angular distribution of the W's to measure the final state W polarization, and then to extract the real and imaginary parts of the form factor from the contribution of $e^+e^- \to W_L^+W_L^-$.

The final state topology with one W decaying hadronically and the other decaying leptonically is best for the analysis. The experimental observables for the polarization analysis are illustrated in Figure 7. They are the W^- production angle (Θ), the polar and azimuthal angles of the lepton in the W rest frame (θ, ϕ), and the polar and azimuthal angles of the quark jets in the W rest frame $(\overline{\theta}, \overline{\phi})$. No quark flavor tagging is assumed so that the two quark directions are averaged over. Events are generated by a Monte Carlo program that retains the full spin correlations through the W decay [29].

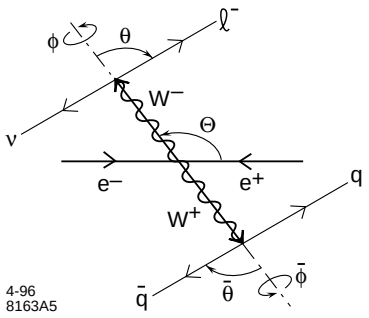

Figure 7: Production and decay angles in $e^+e^- \to W^+W^-$, used for the extraction of the new pion form factor $F_\pi(s)$.

Detector effects are simulated by smearing the four vectors of the final state particles. The analysis uses only two cuts to select events. $|\cos\Theta| < 0.8$ ensures that the event is within the detector volume and the W invariant masses are required to be within a few GeV of the known W mass, where the mass of the leptonically decaying W is reconstructed by using 4-momentum conservation in the event to solve for the 4 vector of the undetected neutrino. The cuts yield a sample that is 98% pure with 36% efficiency (not including the W branching ratios).

The unpolarized differential cross section for $e^+e^- \to W^+W^-$ would be directly sensitive to relatively light vector resonances without any polarization analysis. For example, a ρ_T resonance at the collider center-of-mass energy increases the polarization-summed differential cross section at 90° by a factor of 4. A more challenging question is that of the sensitivity to higher-mass I=1 resonances, or to the LET limit. Figure 8 shows two illustrative determinations of $F_\pi(s)$, through a maximum likelihood fit to simulation data, for the NLC at 1.5 TeV with an unpolarized data sample of 200 fb^{-1}. These determinations are compared to an explicit model with a high-mass vector resonance. The points illustrate the general behavior shown in Figure 3. The LET limit is distinguishable from the case of no new strong interactions at the 4.6 σ level. This translates to a 4.3 σ significance for a 100 fb^{-1} data sample with 80% polarization.

V. THE TOP QUARK COUPLING TO NEW PIONS

In the previous two sections, we have discussed how the new strong interactions responsible for electroweak symmetry breaking are probed by the study of WW scattering, W pair production, and the W gauge couplings. All of these experiments refer only to the property that the new strong interactions spontaneously break $SU(2) \times U(1)$. But the mechanism of electroweak symmetry breaking has one more important task, to give mass to quarks and leptons. It is a very important part of the general program of experiments on the new strong interactions to probe how this sector couples to fermions.

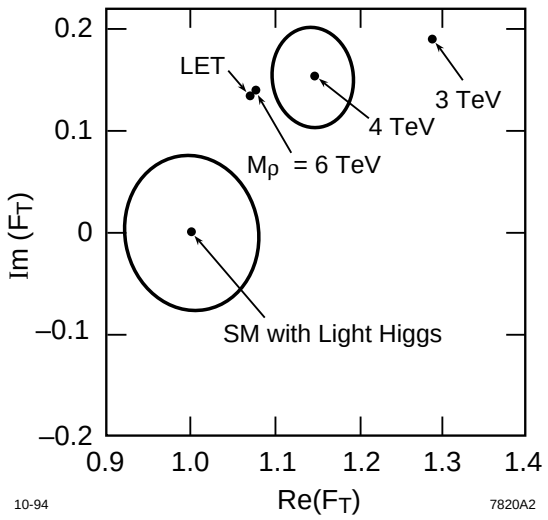

Figure 8: Determination of the new pion form factor $F_\pi(s)$ at the NLC at 1.5 TeV with an unpolarized data sample of 200 fb^{-1}, from [29]. The results are compared to a model with a high-mass ρ_T and LET behavior as this mass goes to infinity. The contour about the light Higgs value is a 95% confidence contour; that about the point $m_\rho = 4$ TeV is a 68% confidence contour.

A particular mystery surrounds the mass of the top quark. This quark must be especially tightly coupled to the new sector. It is tempting to assume that the top quark actually plays an essential role in the mechanism of $SU(2) \times U(1)$ symmetry breaking. It is also possible that new strong interactions of the top quark are shared, to some extent, by the other third generation fermions b and τ. On the other hand, it is equally well possible to have a sector of new strong interactions in which the top quark does not play an essential role.

These different possibilities are reflected in formal considerations for the top quark scattering amplitudes. The low-energy theorem for the process $t\bar{t} \to \pi\pi$, has a steep rise with s similar to that which we discussed for $\pi\pi \to \pi\pi$ in (10) [30, 31, 32],

$$a_0 = m_t\sqrt{s}/16\pi f_\pi^2 + \mathcal{O}(s^2) \,, \tag{16}$$

This formula implies the unitarity bound

$$I = 0 : \ \sqrt{s} < 16\text{TeV} \,. \tag{17}$$

It is an interesting question at what energy the expression (16) turns over to respect unitarity. It could be unitarized by the resonances of the $\pi\pi$ system, at the much lower energies suggested in (12). In this case, the top quark would couple to these resonances as a perturbation, with an amplitude proportional to $(m_t/4\pi f_\pi)$. Alternatively, the $t\bar{t}$ system could couple to new resonances, which might appear either at very high energies or near the TeV scale.

In Section VIII, we will discuss some specific models of fermion mass generation. Within these particular models, there are definite signatures of new physics associated with heavy quarks which can be searched for experimentally. In particular, these models suggest the existence of exotic particles decaying to heavy flavors. We will review searches for these particles in Section IX.

Here we address the question of whether the $t\bar{t}$–$\pi\pi$ amplitude can be directly studied experimentally. The most direct way to do this would be to create top quark pairs by pion-pion scattering. This involves the study of the process $W^+W^- \to t\bar{t}$. The analysis of this process is similar to that of WW scattering. The W bosons are produced by radiation from external fermions lines. There is a contribution from transversely polarized W bosons scattering through the usual standard model interactions. The more interesting contribution from longitudinally polarized W boson may contain enhancements or resonances due to the new strong interactions.

The two most important contributions of the latter type are shown in Figure 9. The coupling of the top quarks and W bosons to a scalar resonance should be proportional to the masses these particles acquire from the Higgs mechanism. Thus, the first diagram of Figure 9 has an amplitude

$$\frac{m_t\sqrt{s}}{f_\pi^2}\frac{M_0^2}{s - M_0^2} \,. \tag{18}$$

This amplitude becomes large for large M_0; in the limit $M_0 \to \infty$, it violates unitarity at high energy. This process is helicity-flip, producing the final states $t_L\bar{t}_L$ and $t_R\bar{t}_R$ predominantly for $s \gg m_t^2$. The second diagram of Figure 9 involves the lowest I=1 (ρ_T) resonance. This resonance has a more model-dependent coupling for which we have introduced a parameter η. The value of the amplitude is

$$\frac{\eta m_t M_1}{f_\pi^2}\frac{s}{s - M_1^2} \,. \tag{19}$$

This process is helicity-conserving, leading to the final states $t_L\bar{t}_R$ and $t_R\bar{t}_L$ at high energy.

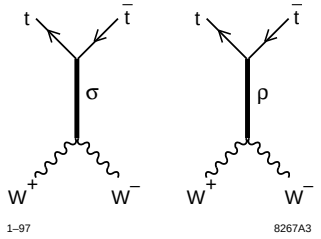

Figure 9: Contributions to $W^+W^- \to t\bar{t}$ from new strong interactions. In this figure, σ is an I=0 resonance; ρ is an I=1 resonance.

Because these two processes lead to different final polarization states of the top quark, it is possible, in principle, to separate them. Each of the two processes gives separate information about the relation of the top quark to the mechanism of $SU(2) \times U(1)$ breaking. For the first process, we can ask, is the

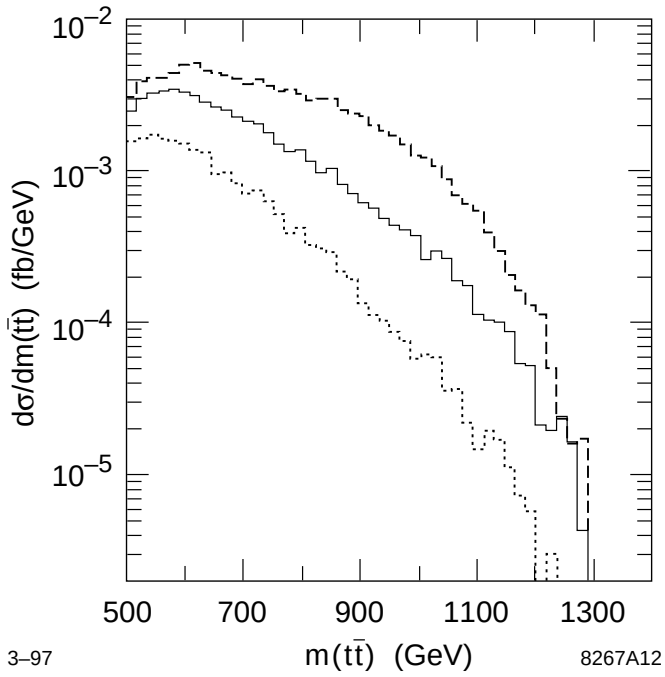

Figure 10: Production cross section for the process $WW \to t\bar{t}$, in the 6-jet topology after all cuts, as a function of the $t\bar{t}$ mass, for a 1.5 TeV NLC with 100% electron polarization, from [28]. The dotted curve is the standard model background; the dashed curve is the effect of a scalar resonance at 1 TeV; the solid curve is the LET prediction.

value of the resonance mass M_0 the same as that observed in I=0 WW scattering? We will describe below a model in which the reaction $WW \to t\bar{t}$ has a lower resonance position, corresponding to a mechanism for generating the top quark mass which is distinct from the mechanism for generating the W mass. For the second process, we can ask, is η close to 1, signaling a significant coupling of the top quark to the I=1 resonance, or is it very small? Thus, even before looking into the details of models, the measurement of this process will give us guidance as the the origin of the top quark mass.

The observation of $WW \to t\bar{t}$ at the LHC seems very difficult due to the overwhelming background from $gg \to t\bar{t}$. However, it appears to be feasible to study this process at the NLC. A simulation study has been done of the reaction $e^+e^- \to \nu\overline{\nu}t\bar{t}$, which contains $WW \to t\bar{t}$ as a subprocess, assuming contributions from an I=0 resonance only [28]. The standard model predictions for this process have been presented in [33]. As in the boson-boson scattering studies at the NLC, it is advantageous to reconstruct the top quarks in their hadronic decay modes. The experimental signature is either 6 jets (two of which are potentially b tagged) or 4 jets and a lepton (again with potentially two b tags). The final jets (and leptons) are kinematically fit to form a $t\bar{t}$ system. The dominant background is two-photon production of $t\bar{t}$ pairs through the process $e^+e^- \to e^+e^-t\bar{t}$. This background can be suppressed by requiring transverse momentum of the $t\bar{t}$ system and a forward electron veto, just as in the analysis of boson scattering processes.

The cross section for the 6-jet topology at the NLC at 1.5 TeV, after all cuts have been applied, is shown in Figure 10. The highest curve is the prediction of a model with an I=0 resonance at 1 TeV. Even in this case, there is no clear resonance shape but only an enhancement above the background. However, the predicted enhancement is significant not only for this example but also for the LET limit. The event yield in that case is given in Table IV.

VI. SUMMARY OF EXPERIMENTAL PROSPECTS AT LHC AND NLC

Now that we have reviewed the major simulation studies of vector boson scattering processes at future colliders, we must try to place the results in a coherent picture. What do these results mean qualitatively? What will we really learn about the new strong interactions from the LHC? What will the NLC add to our understanding?

A. Existence of New Strong Interactions

To begin, let us summarize the results of the previous sections. From the studies of the vector boson scattering, we have seen that the LHC can establish the presence of new strong interactions in the channel $qq \to qqW^{\pm}W^{\pm}$ even at the level of the LET predictions. The estimates in the literature of the experimental significance of such a measurement range from 3.5 to 7 sigma. The most conservative numbers are from the ATLAS Technical Proposal [23] using double jet tagging. The NLC can independently establish the presence of new strong interactions

Table IV: Summary of yields from the LHC and NLC studies described in Sections IV and V, for the LET limit, scaled to 100 fb^{-1} data samples.

Process	N(signal)	N(bkgd)	$S/\sqrt{B}$	ref.
$qq' \to qqW^{\pm}W^{\pm}$	39	76	4.5	[23]
$qq \to qqZ^0Z^0$	10.4	3.3	5.7	[16]
$e^+e^- \to \nu\overline{\nu}Z^0Z^0$	41	50	5.7	[27]
$e^+e^- \to \nu\overline{\nu}t\bar{t}$	53	36	8.8	[28]

in the $e^+e^- \to \nu\overline{\nu}Z^0Z^0$, and $e^+e^- \to \nu\nu t\bar{t}$ channels. A summary of the yields reported in the NLC and LHC studies is given in Table IV. In this table, we have scaled the simulation results presented previously to 100 fb^{-1} data samples, with 80% polarization for the e^+e^- reactions. All of the results that we will present in this section assume the statistics of samples of this size.

In addition, we have discussed the probe of the new strong interactions given by the search for I=1 resonances, or, equivalently, in the study of the new pion form factor. We have seen that the LHC will detect I=1 WZ resonances up to masses of 1.6 TeV. The study of $e^+e^- \to W^+W^-$ at the NLC will be sensitive to the form factor effect even in the LET limit.

Beyond these pieces of direct evidence, the exclusion of a light Higgs boson coupling to ZZ would force us to consider new strong interactions as the only alternative to explain electroweak symmetry breaking.

B. Sensitivity to New Resonances

Demonstrating the existence of new strong interactions, however, is only the first step. In order to build and test models of these new interactions, we will need to obtain the basic experimental information on their structure. In principle, one could imagine going to very high energy and mapping out the structure of resonances of the new strong interactions, as we have done in QCD. However, this is not a realistic goal for the next generation of colliders. We found it interesting to ask a more modest question: Can the colliders of the next generation identify the lowest-lying resonances of the new strong interactions and measure their masses? For example, can the LHC and the NLC distinguish a model in which the new strong interactions are described by quark model, with a strong I=J=1 resonance, from one resembling a strongly coupled Higgs model with a strong I=J=0 resonance and little activity in the I=1 partial wave?

The best way to address this question would be to perform new simulations using a variety of possible strong interaction models. We have not done that in this study. However, we believe that it is possible to reinterpret the results of the simulation studies we have reviewed in Sections IV and V to give a first quantitative answer to this question. We will now discuss three strategies to this conclusion.

1. *Comparison of Models*

The first approach we follow is to ask whether specific models studied by simulation in the literature could be distinguished on the basis of the simulation results. A particularly interesting study for this purpose is that of [16]. This analysis compared the signal strength at the LHC in a variety of channels for five specific models of the new strong interactions: the standard model with a 1 TeV Higgs boson, a model with a scalar resonance at 1 TeV, a model with a vector resonance at 1 TeV, a model with a vector resonance at 2.5 TeV, and a nonresonant model. The first two models differed primarily in the width of the scalar resonance, which was taken to be 0.49 TeV and 0.35 TeV, respectively, in the two cases. In the fifth model, the pion-pion scattering amplitudes were given by the LET with K-matrix unitarization. For each model, the signal strength was computed for a fixed set of experimental cuts. Only the gold-plated modes were considered, and so the yields are rather small.

Given this data, one can ask the question, if these yields are fluctuated statistically, to what extent could the results for one model be fit by one of the other models? This analysis is described in detail in a separate paper in these proceedings [34]. The result is that the first two models are clearly distinguished from the others. Further, these two models give a poor fit to one another, with a χ^2 per degree of freedom greater than 2 for the wrong choice. The models with vector resonances were not distinguished from the LET model. However, this is not a surprise, since these are distinguished from the LET primarily by the search for resonance production via $q\overline{q} \to WZ$, and this reaction is not selected by the cuts of [16]. We have seen that, when the mass of the vector resonance is as low as 1 TeV, it is a prominent feature that would distinguish this model.

2. *Analysis of Yields*

It is possible to go a step further with the data from the simulation studies. To the extent that an experiment can distinguish the LET prediction from the case without new strong interactions, it can also be sensitive to an enhancement of the same signal due to new strong interaction resonances. As a convenient basis for analysis, we might parametrize the new pion scattering amplitudes with simple formulae depending on resonance masses, as we discussed in Section III. Then we can ask, how well can the parameters in these formulae be measured in various reactions.

We can give a rough but quantitative answer to this question for any process in which we understand the accuracy with which the signal of new strong interactions is measured. Thus, we can

estimate the sensitivity to resonances of experiments on boson-boson scattering and on the new pion form factor.

We emphasize that, in this analysis, we are not insisting that the resonance be detected as a peak in the WW scattering cross section. We are asking only whether the resonance can be detected as an excess of events that may be associated with a new strong interaction resonance. The resonance peak may be difficult to detect either because the resonance is very broad (as in the case $m_H = 1$ TeV in Figure 6) or because it is at an energy higher than the parton-parton center-of-mass energy (the typical situation for an I=1 resonance which gives a small enhancement to the new pion form factor). If there are two important resonances in a scattering channel, the effective mass parameter will be a combination of the two masses. It is also possible that two resonances in a single channel could destructively interfere at low energy and produce no observable effect. Nevertheless, we feel it is interesting to ask how well the data from future colliders will determine one parameter for each partial wave beyond the model-independent scattering lengths given in (11).

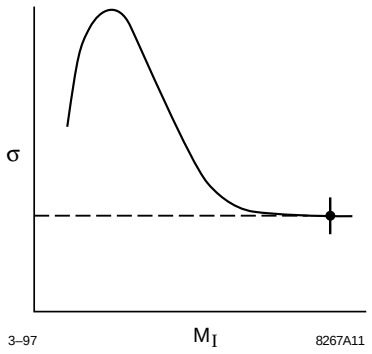

Figure 11: Cross section for the process $\pi\pi \to \pi\pi$ in a given partial wave, at fixed $\pi\pi$ center-of-mass energy, as a function of the mass M of a resonance in this channel.

Consider first the case of boson-boson scattering. In Figure 11, we show a typical $\pi\pi$ scattering cross section at fixed $\pi\pi$ center-of-mass energy, as a function of the resonance mass M_I defined in (14), with I taken to be the dominant partial wave for this reaction. The cross section peaks at the value of M_I equal to the center-of-mass energy used. If M_I is much larger than the center-of-mass energy, the resonance recedes and the cross section decreases. As $M_I \to \infty$, the cross section approaches a limiting value; this is precisely the LET model.

For each simulation study in Table IV, we have the expected number of signal and background events for the case in which the $\pi\pi$ scattering process is governed by the LET model. From the quoted yields in each simulation, and assuming that the dominant source of error is the statistical fluctuation of the small number of signal and background events, we can compute the accuracy with which the predicted LET cross section is measured. Then, assuming that we know the shape of the cross section curve with M_I, we can ask: (1) At what value of M_I does an event excess appear at the 95% confidence level? (2) At a given value of M_I at the upper end of the observable range, what is the uncertainty in the determination of M_I from the event excess?

To answer these questions, we made several further simplifications. We did not redo the simulations to compute the dependence of the cross sections on M_I. Rather, we used the dependence on M_I of scattering cross sections at the $\pi\pi$ center-of-mass energy equal to the typical value 1 TeV. For the reactions $WW \to ZZ$, which receive contributions from I=0,2, we assumed that the resonance producing the event excess was in the I=0 channel. This can be checked by looking for an event excess in $W^+W^+ \to W^+W^+$, which contains only I=2. For $WW \to t\bar{t}$, we assumed that the resonance was in the I=0 channel. In principle, that could be checked by t quark helicity analysis, as we have explained in Section V.

We have displayed the results of this analysis in the fourth and fifth columns of Table V. We also show in this table results for the annihilation reactions $q\overline{q} \to WZ$, $e^+e^- \to W^+W^-$. In the $q\overline{q}$ annihilation process, the signal is a narrow resonance peak. We have quoted in the last column our estimate of the width of this peak close to where it disappears into the background. For the e^+e^- annihilation process, we have estimated the mass sensitivity from the results of [29], assuming a vector meson dominance parametrization for the new pion form factor.

3. Effective Lagrangian Studies

Two studies done for Snowmass used an effective chiral Lagrangian to parametrize the $\pi\pi$ scattering amplitudes [20, 21]. They then reported constraints on the parameters of the chiral Lagrangian that could be obtained at future colliders. Though these analyses use a different language that the one we have used up to this point, it is instructive to convert their results to our parametrization where this can be done simply, in order to check the results of the previous subsection.

The effective Lagrangian method introduces as its variable an $SU(2)$ unitary matrix U. The expectation value of this matrix is nonzero if $SU(2)$ is spontaneously broken. The matrix U is related to the pion field by

$$U = e^{-i\pi^a\sigma^a/2v}, \tag{20}$$

where v is given by (8). The most general Lagrangian function of U which is invariant under $SU(2) \times SU(2)$ chiral symmetry is [17]

$$\begin{aligned}\mathcal{L} &= \frac{v^2}{4}\mathrm{tr}[\partial_\mu U^\dagger \partial^\mu U] + L_1\left(\mathrm{tr}[\partial_\mu U^\dagger \partial^\mu U]\right)^2 \\ &\quad + L_2\left(\mathrm{tr}[\partial_\mu U^\dagger \partial_\nu U]\right)^2 + \cdots,\end{aligned} \tag{21}$$

where the omitted terms contain at least six derivatives. The $\pi\pi$ scattering amplitudes derived from (21) do not respect unitarity, but they are properly crossing symmetric. The terms proportional to L_1 and L_2 give the most general terms of order s^2 which can be added to (10) in a chirally invariant theory. In [21], the parameters L_1 and L_2 are called α_5 and α_4.

By comparing this parametrization to (14), one can work out the relation between L_1 and L_2 and the masses M_0 and M_1 in

Table V: LHC and NLC sensitivity to resonances in the new strong interactions. 'Reach' gives the value of the resonance mass corresponding to an enhancement of the cross section for boson-boson scattering at the 95% confidence level obtained in Section VIB2. 'Sample' gives a representative set of errors for the determination of a resonance mass from this enhancement. 'Eff. $\mathcal{L}$ Reach' gives the estimate of the resonance mass for a 95% confidence level enhancement obtained in Section VIB3. All of these estimates are based on simple parametrizations in which a single resonance dominates the scattering cross section. A more complete explanation of the assumptions used is given in the text.

Machine	Parton Level Process	I	Reach	Sample	Eff. $\mathcal{L}$ Reach
LHC	$qq' \to qq'ZZ$	0	1600	1500^{+100}_{-70}	1500
LHC	$q\overline{q} \to WZ$	1	1600	1550^{+50}_{-50}	
LHC	$qq' \to qq'W^+W^+$	2	1950	2000^{+250}_{-200}	
NLC	$e^+e^- \to \nu\overline{\nu}ZZ$	0	1800	1600^{+180}_{-120}	2000
NLC	$e^+e^- \to \nu\overline{\nu}t\overline{t}$	0	1600	1500^{+450}_{-160}	
NLC	$e^+e^- \to W^+W^-$	1	4000	3000^{+180}_{-150}	

that formula. When L_2=0, this relation takes the simple form

$$M_0^2 = \frac{v^2}{8L_1}\,. \tag{22}$$

Then we can convert the results of these papers to our terminology as follows. Peláez [20] studied the reaction $qq \to qqZZ$ at the parton level following the scheme of cuts of the CMS collaboration [22]. He found that the 95% confidence upper limit on L_1 in the LET was about 3.5×10^{-3}. Kilian [21] studied the reactions $e^+e^- \to \nu\overline{\nu}ZZ$ and $e^+e^- \to e^+e^-W^+W^-$ at the parton level for a 1.6 TeV e^+e^- collider, following the scheme of cuts suggested in [27]. His results were presented for 200 fb^{-1} and unpolarized beams; scaling to 100 fb^{-1} and 80% polarization, we find a 95% confidence upper limit on L_1 of about 1.8×10^{-3}. Converting these values to limits on M_0, we find the two entries in the extreme right-hand column of Table V.

4. Results

We were surprised at the quality of the information that the set of experiments shown in Table V will make available. The experiments are sensitive to resonances in each of the three partial waves available to new pion scattering, up to resonance masses significantly larger than the unitarity limits shown in (12). We have discussed many qualifications of this analysis, most importantly, our assumption that a single resonance dominates each partial wave. However, under the assumptions we have made the masses of the resonances are obtained to 10-15%. And it is possible to test whether an I=0 resonance which appears in $WW \to t\overline{t}$ is the same one that appears in $WW \to ZZ$.

C. Further Questions

There are many questions that still must be addressed, and which require analysis beyond the level possible in a summer study. We list the most important open issues here.

First of all, the analysis we have done to determine the sensitivity to resonance masses of the new strong interactions should be repeated using detailed simulations, at least at the parton level, to produce the correct average over $\pi\pi$ reactions of different center-of-mass energy.

For the LHC studies, two major questions could benefit from future work. Since the $\pi\pi$ scattering signals are seen as event excesses above background, it is necessary that the backgrounds be estimated confidently. Backgrounds which depend on missing transverse momentum and thus on cracks and gaps in the detector need experimental calibration. In addition, the efficiencies of jet tags and jet vetos must be determined experimentally, and strategies are needed to do this.

In addition, we feel it is important to extend the LHC simulation studies beyond the study of the lowest-background 'gold-plated' modes. Once the existence of new strong interactions has been established and we are interested in measuring parameters of the new strong sector, it will be important to have probes of this sector that allow higher-statistics measurements even at the cost of new uncertainties in backgrounds. More work is required on studies of the 'silver-plated' modes, with one leptonic and one hadronic weak boson decay, with forward jet tagging. CMS has already shown promising results in a 1 TeV Higgs search with this strategy. Another means of controlling background is to associate WW scattering events with rapidity gaps or other measures of low central hadronic multiplicity. Here it seems especially important to find a way to calibrate the tag experimentally.

For the NLC studies, though we believe that the major effects which determine the experimental yields and resolutions have been taken into account, it would be best to repeat the analyses of boson-boson scattering using realistic simulations of hadronization, detector effects, and beamstrahlung. These simulations could also be used to explore additional observables available at the NLC, in particular, the use of W and Z helicity analysis such as we discussed for annihilation processes in Section IVC2. Positron polarization would also enhance the capabilities of the NLC, and this should be studied.

In addition, it is interesting to think about the desired energy of a future lepton collider. The case of a 4 TeV e^+e^- or $\mu^+\mu^-$ collider has been studied [35] and, not surprisingly, it provides significant increases in the projected signals over those available from LHC or the 1.5 TeV NLC. We will see on what time scale this technology could become available. For the near term, there is a question whose answer is less obvious: Would we gain from extending the reach of the 1.5 TeV e^+e^- collider to 2 TeV with an attendant loss in luminosity? The optimization of energy versus luminosity for boson-boson studies with e^+e^- colliders needs further study.

D. Issues for Very High Energies

At the beginning of Section VIB, we stated that the detailed mapping of the resonances in the new strong interactions was not a realistic goal for the next generation of colliders. However, if there are new strong interactions, we will eventually need to face this problem. To our knowledge, this issue has received almost no consideration, even though it may become the major focus of experimental particle physics two decades from now.

At an e^+e^- or $\mu^+\mu^-$ collider, the problem of mapping resonances is relatively straightforward. If the constituents of the new strong interactions have $SU(2)\times U(1)$ charges, which they must to produce electroweak symmetry breaking, the J=1 resonances of this sector will appear in lepton-antilepton annihilation. To study these resonances, one needs the ability to produce data samples which grow as the square of the energy; for example, samples of 1000 fb^{-1} are needed at $\sqrt{s}$ = 5 TeV. The new resonances presumably decay dominantly to new pions, that is, to W and Z bosons. The most direct experimental strategy would be to identify these bosons in their hadronic decay modes by making 2-jet mass combinations. This raises an interesting question: In e^+e^- reactions at present energies, annihilation processes at the full $\sqrt{s}$ can be distinguished from two-photon processes and other peripheral reactions by cuts on total energy and visible transverse energy. Does this strategy continue to work at center-of-mass energies of order 5 TeV when one includes the new sources of gauge boson production from photon-photon collisions and direct W and Z radiation? This question should be studied in simulations.

For a pp collider at 100 TeV in the center of mass, it is less obvious what the strategy would be to explore the resonance region of the new strong interactions. The one part of this question that has been addressed in the literature is that of the observability of multiple W production due to new strong interactions [36, 37]. A 100 TeV collider would allow boson-boson collisions at energies corresponding to the multiple pion production region of QCD. In a preliminary study at Snowmass, Kilgore and Peskin asked whether the multiple production of new pions (observed as W and Z bosons with p_T above 500 GeV) would be visible over standard model backgrounds. Because it decreases the rate too much to insist that all of the weak bosons decay leptonically, most of the weak bosons must be identified in their hadronic decay modes and thus will resemble high p_T jets. The dominant backgrounds come from QCD production of W or Z plus multiple gluon jets. The signature is the presence of events with high jet multiplicity per unit rapidity, with $dn/dy \sim 3$ for new pion production versus $dn/dy \sim 0.2$ for the standard model reaction. They estimated that a data sample of order 1000 fb^{-1} would be necessary to study this process. If QCD is a guide, the study of the truly short distance regime of the new strong interactions would presumably require several further orders of magnitude in luminosity.

This analysis gives one example of the type of question that will need to be addressed to define the experimental program of these very high energy colliders. The formulation of this experimental program is clearly at an early stage.

VII. ANOMALOUS W COUPLINGS

Up to this point, we have discussed probes of the new strong interactions through scattering processes of new pions. An alternative way to probe these new interactions is to study their effect on the couplings of W and Z bosons. For example, the standard Yang-Mills coupling of the W boson to the photon may be modified by

$$\Delta\mathcal{L} = e\left[\left(W^\dagger_{\mu\nu}W^\mu - W^{\dagger\mu}W_{\mu\nu}\right)A^\nu + \kappa_\gamma W^\dagger_\mu W_\nu F^{\mu\nu} + \cdots\right] \tag{23}$$

The standard Yang-Mills coupling is given by $\kappa_\gamma = 1$. A deviation of κ_γ from this value signals an anomalous magnetic moment for the W boson. The complete phenomenology of the possible modifications of this form is described in the contribution [38] to these proceedings. Here, we will make only a few general remarks which connect that study with the theory of pion-pion interactions.

To understand how new pion interactions affect the W and Z couplings, the most straightforward method is to write the most general effective Lagrangian for pions coupled in a gauge-invariant way to $SU(2)\times U(1)$. Some time ago, Gasser and Leutwyler [17] addressed this problem for the conventional strong interactions, considering arbitrary vector bosons coupling to the $SU(2)\times SU(2)$ global symmetry. Using the analogy between QCD and the new strong interactions, and specializing their results to the standard model gauge couplings, one finds as the leading corrections [39, 40]

$$\begin{aligned}\delta\mathcal{L} &= -iL_{9L}\epsilon^{abc}gW^a_{\mu\nu}\partial^\mu\pi^b\partial^\nu\pi^c \\ &\quad -iL_{9R}\epsilon^{3bc}g'B_{\mu\nu}\partial^\mu\pi^b\partial^\nu\pi^c \\ &\quad +L_{10}B_{\mu\nu}W^{\mu\nu 3},\end{aligned} \tag{24}$$

where $a,b,c = 1,2,3$ and $W^a_{\mu\nu}$, $B_{\mu\nu}$ are the field strength tensors of $SU(2)$ and $U(1)$ gauge fields, and the L_i are new phenomenological parameters. As shown in Figure 12, the first two

terms of (24) can be thought of as resulting from new strong interactions at the gauge boson vertex. The third term can be thought of as the contribution to the vacuum polarization resulting from virtual states of the new sector.

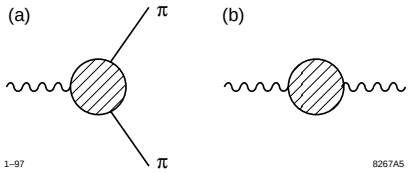

Figure 12: Corrections to gauge boson vertices from new strong interactions.

To understand the importance of the new couplings introduced in (24), we should first estimate the L_i and then relate these parameters to quantities such as κ_γ that express the corrections to the $WW\gamma$ and WWZ vertices. The simplest way to estimate the L_i is to saturate the strong interaction amplitudes shown in Figure 12 with low-lying resonances. Since this is just an estimate, we will assume for simplicity that the new strong interactions conserve parity; this sets $L_{9L} = L_{9R}$. Then, if M_1 is the mass of the lowest I=1 vector resonance,

$$\begin{aligned} L_9 &= \frac{1}{2}\frac{f_\rho^2}{M_1^2} \\ L_{10} &= -\frac{1}{2}\frac{f_\rho^2}{M_1^2}\left(1 - \frac{f_\rho^2 M_1^2}{f_A^2 M_{A1}^2}\right) \end{aligned} \qquad (25)$$

where M_{A1} is the mass of the lowest I=1 axial vector resonance. In a more sophisticated estimate, these expressions would be replaced by dispersion relations over the spectrum of vector and axial vector mesons [17, 4].

The parameter L_{10} is actually already known, since it is related to the S parameter of precision electroweak physics, by

$$L_{10} = -\frac{1}{16\pi} S \,. \qquad (26)$$

The value of S given in (3) leads to $L_{10} = +(5\pm3)\times10^{-3}$. This would seem to imply an unconventional ordering or degeneracy of the vector and axial vector mesons of the new sector relative to the quark model expectation.

Given values for the L_i, the parameters κ_γ and κ_Z expressing the corrections to the $WW\gamma$ and WWZ vertices are given by

$$\begin{aligned} \kappa_\gamma &= 1 - 4\pi\alpha_w \cdot \frac{1}{2}\big(L_{9L} + L_{9R} + 2L_{10}\big) \\ \kappa_Z &= 1 + 4\pi\alpha_w \big(L_{9L} - \frac{\sin^2\theta_w}{\cos^2\theta_w} L_{9R} \\ &\qquad + \frac{2}{\cos^2\theta_w} L_{10}\big) \,. \end{aligned} \qquad (27)$$

In addition, the overall strength of the WWZ vertex is shifted by a factor

$$g_{1Z} = +4\pi\alpha_w \cdot \left(\frac{1}{2\cos^2\theta_w} L_{9L} + \frac{\sin^2\theta_w}{\cos^2\theta_w(\cos^2\theta_w - \sin^2\theta_w)} L_{10}\right) . \qquad (28)$$

In the previous section, we argued that the pion-pion scattering effects can show up in the new pion form factor. In cases where this form factor does not contain a resonance and we observe just the first deviation from its low-energy value, this deviation is a special case of the couplings described in this section. Specifically,

$$\text{Re } F_\pi(q^2) = 1 + \frac{s}{f_\pi^2}\,(L_{9L} + L_{9R}) + \mathcal{O}(s^2) \,. \qquad (29)$$

(The imaginary part of F_π is generated by loop corrections to the pion effective Lagrangian.)

If we estimate L_{9L}, L_{9R} by evaluating (25) with the parameter values of QCD, and we ignore L_{10} in accord with the electroweak data, we find

$$\kappa_\gamma - 1 \sim -3\times10^{-3} \qquad \kappa_Z - 1 \sim -2\times10^{-3} \,. \qquad (30)$$

Experiments which claim to probe new strong interactions through the anomalous W couplings should be designed to achieve a level of accuracy which would be sensitive to such small corrections.

Many studies have been done to explore the sensitivity of current, future, and proposed machines to anomalous gauge boson couplings. The recent DPF study of physics beyond the standard model presented the summary of the sensitivity of future colliders to the anomalous couplings shown in Figure 13 [41]. These limits are based on a specific two-parameter representation of the anomalous couplings [42], but they illustrate well the constraints that will be available. The studies presented at Snowmass [38] have refined the limits presented in the figure but do not significantly change the projections. From a comparison of (27) and Figure 13, we see that anomalous couplings are not particularly sensitive probes of new strong dynamics. The only machine that will have sufficient sensitivity to probe the new strong interactions through the anomalous W coupling is the e^+e^- linear collider, with a study of the helicity amplitudes in $e^+e^- \to W^+W^-$. However, this is the same analysis and the same data that yield a measurement of the phase shift in the I=1 weak isospin channel and gives direct evidence for strong scattering. Our conclusion is that while experiments searching for anomalous gauge boson couplings are extremely important as tests of the standard model, they are not sensitive probes of strong-coupling electroweak symmetry breaking.

VIII. FERMION MASSES AND MODEL-DEPENDENT SIGNATURES

Up to this point, we have been concerned with the general phenomenology of strong interactions associated with electroweak gauge symmetry breaking. We have discussed experimental probes of these new strong interactions which apply irrespective of their detailed properties and which give the most important qualitative information about their structure. Any successful theory of electroweak symmetry breaking, however, must *also* explain the origin of the masses of the ordinary

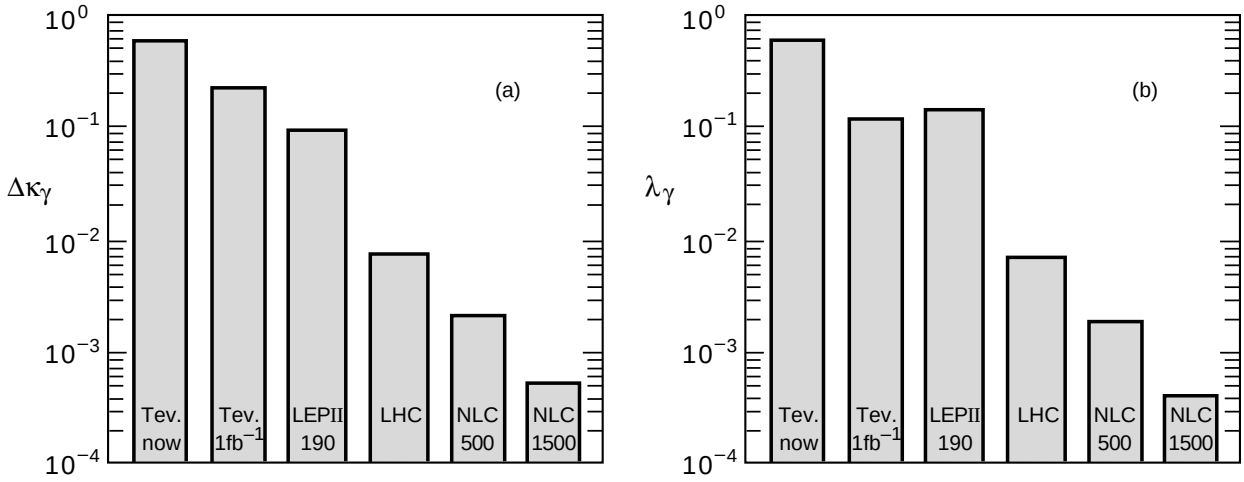

Figure 13: Comparison of 95% confidence limits on the anomalous $WW\gamma$ couplings (a) κ_γ and (b) λ_γ expected from various future colliders, from [41].

fermions. The mechanism of fermion mass generation typically leads to the prediction of new particles and interactions with the property of coupling most strongly to heavy flavors. In this section, we will discuss model-dependent experimental signatures of these new interactions. The effects we will review are associated with specific features of models, and so we cannot be sure that experiments which may exclude these effects give general constraints on electroweak symmetry breaking and fermion mass generation. However, we will see that explicit models of fermion mass generation often can be probed in ways quite different from the high-energy pion-pion reactions that we have discussed up to this point.

This section is built around a description of two features which may be incorporated into models of strong interaction electroweak symmetry breaking with fermion mass generation: walking technicolor and top quark condensation. We will briefly outline the motivation of these ideas and show how, in each case, the basic theoretical assumptions give rise to new observable phenomena. To introduce this discussion, we review the minimal model of technicolor, the simplest scenario for electroweak gauge symmetry breaking and fermion mass generation, which is ultimately unsuccessful. We will find the more realistic models by repairing the difficulties of this one.

The concentration of this section on one particular route to model-building may reflect the primitive state of our knowledge of nonperturbative phenomena in gauge theories, which provide the theoretical raw materials for model construction. Thus, it is important to look at the effects discussed in this section as examples of what might be found rather than predictions of the general notion of strong-coupling electroweak symmetry breaking. Eventually, experiments will tell us whether our current theoretical ideas are good enough, or whether they must be expanded.

A. Technicolor and Extended Technicolor

The ideal model of new strong interactions responsible for $SU(2) \times U(1)$ is technicolor [43, 44]. In this model, one postulates a new set of interactions with exactly the physics of QCD, but with QCD scale Λ set several thousand times larger in accord with (8). If the model contains two flavors of massless 'techniquarks' T, it has $SU(2) \times SU(2)$ global symmetry. This symmetry is spontaneously broken in the correct pattern through quark pair condensation and dynamical mass generation, exactly as happens in the familiar strong interactions.

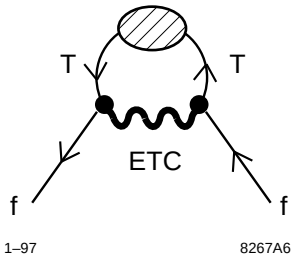

Figure 14: Generation of quark and lepton masses through extended technicolor interactions.

Masses for quarks and leptons must be induced by additional interactions that couple these fermions to the techniquarks. A plausible hypothesis is that these couplings result from further new gauge interactions, called 'extended technicolor' (ETC) [45, 46]. The theory then produces quark and lepton masses proportional to the dynamical mass of the techniquarks, through the diagram shown in Figure 14.

Though this scenario is simple and compelling, it cannot be correct. It has two difficulties associated with the ETC mechanism, and one associated with precision electroweak results.

First, since the ETC interactions must distinguish between flavors, the ETC gauge group typically contains vector bosons that couple to the first two generations and mediate flavor changing neutral current processes such as K^0–$\overline{K}^0$ mixing, at an unacceptable level [45, 47, 48]. Though these bosons are very heavy, typically in the mass range of 50 TeV, the constraints on flavor-changing neutral currents are very stringent. Second, the ETC mechanism cannot give a large mass to the top quark without fine-tuning [49, 50]. For top quark masses above about 100 GeV, the mass of the required ETC boson comes down to about 1 TeV, where this particle would play a role in the technicolor dynamics and, in particular, spoil custodial $SU(2)$ symmetry. Finally, because this theory is a scaled-up version of QCD, the value of S conflicts with precision electroweak results as we have discussed above.

Despite these problems, many authors have viewed technicolor as a reasonable starting point for a theory of electroweak symmetry breaking induced by new strong interactions. The question is, what should be changed so that this mechanism avoids its specific problems? We now consider two possible answers.

B. Walking technicolor

Much of the analysis above is based on our understanding of QCD. As one scales higher in energy, QCD goes rather suddenly to a weakly coupled theory due to asymptotic freedom. The first proposal, "walking technicolor" [51, 52, 53], assumes that the short-distance behavior of the technicolor interactions is instead dominated by an ultraviolet fixed point. In this case, or even if the approach to asymptotic freedom is very slow [54], the dynamics of the strong interactions could be quite different.

Recently, it has been found that the supersymmetric generalization of QCD, for a large number of quark flavors, has a nontrivial fixed point with a manifold of vacuum states, including a point at which chiral symmetry is unbroken [55]. In walking technicolor, we hope that either an approximate [56] or exact fixed point governs the asymptotic ultraviolet behavior of ordinary, nonsupersymmetric, QCD with a large number of flavors, or with matter in some nonstandard gauge representation. However, to obtain electroweak symmetry breaking, we must also assume that chiral symmetry is broken according to the standard pattern.

The consequences of the new short-distance behavior may include nonperturbative short-distance enhancements of amplitudes which involve expectation values of techniquark bilinears. In particular, the process shown in Figure 14 is enhanced, pushing up the general scale of ETC bosons and thus suppressing the dangerous flavor-changing neutral current amplitudes involving the first two generations.

This proposal has important experimental consequences. If the short-distance behavior of technicolor is due to the presence of many technifermions, this predicts the existence of additional pseudoscalar mesons which are composites of the techniquarks. In QCD, when we consider a theory with a light strange quark, we add to the pion isotriplet the kaons and the eta; similarly, a generalization of QCD with n flavors leads to (n^2-1) meson species, including the three pions. The new particles are known as 'technipions' or 'pseudo-Goldstone bosons' P.

In models where techniquarks carry QCD color, we can form technicolor singlet mesons which carry QCD color, for example, by combining two colored techniquarks into a technicolor-singlet, color-octet combination. However, in all models, some techniquarks must transform under weak interaction $SU(2)$ and custodial $SU(2)$, and therefore the additional mesons can form isospin doublets, triplets, and possibly also higher isospin representations. For example, a model which contains three doublets of technifermions which transform as color triplets (U, D) predicts 35 meson states: 3 pions and an isotriplet of color octets P^{a+}, P^{a0}, P^{a-}, and a color octet isosinglet $P^{a0\prime}$. The ETC-interactions associated with the top quark mass would allow these particles to decay preferentially to third-generation fermions pairs such as $t\bar{t}$, $t\bar{b}$, and $t\tau$.

The technipion masses come from two sources. First, there is a contribution from standard model gauge interactions. This is the technicolor analogue of the π^+–π^0 mass difference; its value is about 300 GeV for colored states [57]. Second, there is a contribution from ETC interactions of the techniquarks inside the mesons. This contribution is small in conventional technicolor, but in walking technicolor it receives a double enhancement and is expected to be the dominant contribution [51]. Unfortunately, this contribution cannot be accurately calculated even in the simplest realistic models.

If the technicolor model contains techniquarks in higher technicolor representations, it is possible that the techniquarks might have significantly different values of their dynamical masses. That is, these models may contain multiple, and significantly different, scales of chiral symmetry breaking [58, 59, 60]. Models with "multiscale technicolor" have the general experimental signatures of walking technicolor models, necessarily including large multiplets of technipions. In addition these models contain relatively light I=1 resonances, the ρ resonances in the sectors of the theory associated with the lowest chiral-symmetry breaking scale. These resonances, which may be as light as 500 GeV [59], can be produced in fermion-antifermion annihilation as discussed above and provide enhancements in the cross sections for W^+W^- and P^+P^- production at relatively low energies.

Finally, as emphasized by Lane [61], the estimate of S which we have given in Section IIA depends crucially on the assumption that the new strong dynamics is QCD-like. We have explained in Section VII how a different hadron spectrum can lead to a vanishing or negative value. Unfortunately, it is not known whether a walking technicolor model can in fact have the spectrum required.

While walking technicolor mitigates the flavor-changing neutral-current problems which arise in generating the masses of the first two generations of quarks, it does not address the problems associated with a heavy top quark. In the absence of fine-tuning [62], the ETC boson associated with the top quark would still have a mass of order 1 TeV [63], and in fact, the new asymptotic behavior tends to enhance isospin-violating effects [64]. An additional potentially dangerous consequence of a light ETC gauge-boson is the presence of anomalous cou-

plings of the third-generation quarks. The ETC gauge group includes gauge bosons which modify the t and b vertices with the Z^0 through the processes shown in Figure 15. These diagrams have been estimated [65] and turn out to be of order

$$\delta g_Z \sim g_Z \cdot \frac{m_t}{4\pi f_\pi} , \tag{31}$$

giving corrections of order 7%. Note that this contribution involves only one power of (m_t/f_π), whereas most vertex corrections due to top quark mass generation are suppressed by two powers of this ratio. In explicit models [66, 67, 68], the contributions from standard and diagonal ETC bosons shown in the figure are of opposite sign for b and of the same sign for t, so one expects a few-percent and rather model-dependent effect on $\Gamma(Z^0 \to b\overline{b})$ but effects of order 10% for the top quark couplings [69, 70].

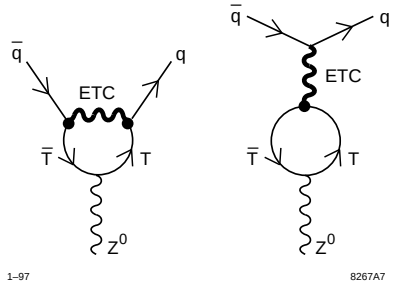

Figure 15: Modification of the $b\overline{b}Z$ and $t\overline{t}Z$ vertices by ETC interactions.

The final consequence of this class of models is the prediction of heavy particles which are bound states of techniquarks with the light ETC boson associated with top quark mass generation [71, 72]. These states have the quantum numbers and decay schemes of excited third-generation fermions, for example,

$$t^* \to tZ,\ bW , \qquad \tau^* \to \tau Z,\ \nu_\tau W . \tag{32}$$

C. Topcolor-Assisted Technicolor

To address the problems discussed at the end of the previous section, one might introduce a new interaction specifically associated with the top quark, in order to generate its large mass by top quark pair condensation. Such new interactions, introduced originally by Hill [73, 74], are called 'topcolor'. Though it is a very attractive idea that top quark pair condensation is the mechanism of $SU(2) \times U(1)$ symmetry breaking, this is unlikely because the asymmetry between the top and bottom masses would require a large violation of custodial $SU(2)$. To avoid this problem without fine-tuning, the top condensation must be isolated from the technicolor interactions which are the major source of the W and Z masses. This puts the top condensation in an additional new sector, with its own characteristic phenomenology.

The strength of the top condensate is bounded above by a constraint associated with the permitted violation of the relation (1) and is bounded below by limits on the strength of the top quark coupling to new interactions [74]. For simplicity, the interactions which induce top quark condensation are often modeled by 4-fermion contact interactions induced at a scale M of order one TeV. It may be more realistic to assume that the top quark couples to a new sector of (broken) gauge interactions. The strength of these new interactions must be adjusted to be quite near the threshold for chiral symmetry breaking; otherwise, the top quark mass jumps up to the scale of the new interactions (of order one TeV). Direct experimental searches for these gauge bosons as resonances in the $t\overline{t}$ mass distribution push their masses above 600 GeV. Under these constraints, one finds a small contribution to the W mass from top quark pair condensation; this must be supplemented by a larger contribution due to technicolor. Thus, (8) is generalized to

$$f_t^2 + f_\pi^2 = (246\ \text{GeV})^2 , \tag{33}$$

where f_π is the pion decay constant of technicolor and f_t is a new decay constant associated with the top condensate. Typical values are $f_t = 75$ GeV, $f_\pi = 235$ GeV, so that

$$r_t = (f_t/f_\pi)^2 \approx \frac{1}{10} . \tag{34}$$

In addition to the direct manifestations of new top interactions, there is an interesting indirect consequence of this new physics. To the extent that the top condensation is decoupled from the symmetry-breaking of the technicolor fields, the top condensate would lead to its own separate set of Goldstone bosons, the 'top-pions' π_t^+, π_t^0, π_t^-. These receive masses which are small compared to the topcolor scale as the result of the coupling of the top and bottom quarks to technicolor through ETC interactions. However, since ETC now plays only a small role in giving the top quark a mass, these effects are suppressed. If the ETC contribution to the top quark mass is of order 5–10 GeV, the top-pions are expected to have a mass between 150 and 400 GeV [74].

Furthermore, if the top condensate is induced by short-ranged strong-interactions adjusted to be near the critical point for chiral symmetry breaking, the theory predicts a $t\overline{t}$ composite scalar with a mass close to the $t\overline{t}$ threshold [75]. The effective size of this composite system, however, is M^{-1}, which means that for practical purposes this scalar should be treated as an elementary scalar field which we might call the 'top-Higgs' h_t^0. Thus, topcolor leads naturally to the appearance of an additional sector of apparently elementary Higgs bosons.

From this general outline of topcolor models, we can deduce three experimental consequences. First, topcolor gives a potential for resonances in $t\overline{t}$ and $b\overline{b}$ production at high energy. If the topcolor interactions are a new gauge sector, composed of 'top-gluons' with an enhanced coupling to the third generation, these should produce resonances in the reaction $q\overline{q} \to t\overline{t}$. In addition, realistic topcolor models contain a weakly coupled $U(1)$ gauge boson Z_t^0 which distinguishes the t and b. In order to cancel anomalies, this gauge boson will also couple to leptons. Thus, it is likely to lead to resonances or interference effects in all channels of $e^+e^- \to f\overline{f}$, just as for any other type of heavy neutral vector boson.

Second, as we have discussed above, topcolor predicts a top-Higgs sector, a set of four bosons π_t^i, h_t^0 which behave like a second scalar doublet in a multi-Higgs model. The masses of these particles are expected to be in the range 150-400 GeV. Some of their properties are those expected for conventional multi-Higgs models, but some are different in an interesting way. The pair production processes

$$e^+e^- \to \pi_t^+\pi_t^- \ , e^+e^- \to \pi_t^0 h_t^0 \tag{35}$$

have the standard cross sections for an elementary scalar doublet. The process

$$e^+e^- \to Z^0 h_t^0 \ , \tag{36}$$

however, occurs at a rate suppressed from the standard model rate for $e^+e^- \to Z^0h^0$ by a factor r_t in (34). On the other hand, the single production processes

$$\gamma\gamma,\ gg \to h_t^0, \tag{37}$$

are enhanced parametrically relative to the rate for a minimal Higgs boson by a factor $1/r_t$. Further aspects of the physics of these particles are discussed in [76].

The third consequence of topcolor is a suppression of the process $WW \to t\bar{t}$ discussed in Section V. In the I=0 amplitude (18), the mass M_0 of the scalar resonance should be replaced by the mass of the h_t^0, giving a much lower resonance position followed by a rapid fall-off. In the I=1 amplitude (19), the parameter η should be small, of order (m_b/m_t), that is, of the order of the fraction of the top quark mass due to ETC and not topcolor interactions. Topcolor provides a concrete example of the claim we made in Section V, that the cross section for $WW \to t\bar{t}$ tests directly whether the top quark derives its mass from the new strong interactions that produce the W mass, or from some other source.

IX. EXPERIMENTAL SEARCHES FOR EXOTIC PARTICLES

In this section, we summarize the experimental reach of various machines to exotica that are associated with specific models of strong interaction electroweak symmetry breaking. The number of models is large and explicit studies have not been done for all of them. We attempt here to give general guidelines for the experimental reaches rather than report exhaustively for each conceivable model. We consider the search reach of the Tevatron in Run I (0.1fb^{-1}), Run II (2fb^{-1}), and TeV33 (30fb^{-1}), the search reach of an electron-positron linear collider (NLC) at 0.5TeV (50 fb^{-1}), 1.0TeV (100fb^{-1}), and 1.5TeV (100fb^{-1}), and the search reach of the LHC (100fb^{-1}).

A. Technipions

The technipions in a given model can be electrically charged or electrically neutral, and they can exist as color singlets, triplets, or octets. At lepton colliders, the electrically charged technipions are pair produced and can be detected almost up to the kinematic limit of the machine ($\sqrt{s}/2$). The current experimental limits are from the OPAL experiment at LEP1: $m(P^\pm) > 35$ GeV and $m(P_8^\pm) > 45$ GeV [77]. Searching for the neutral technipions at a lepton collider is a bit more subtle. There are no tree level gauge couplings so the neutral technipions are produced via a triangle diagram in association with a monoenergetic gluon, photon or Z. The production cross sections can be sizeable for neutral technipions of mass a significant fraction of $\sqrt{s}$. Swartz has described the search technique in a paper in these proceedings [78]. A 1 TeV linear collider has a mass reach of approximately 700 GeV for the neutral color octet technipion states.

The Tevatron is currently sensitive to the colored technipion states (charged and neutral) only to a mass of 225 GeV [79]. For a neutral, color octet technipion arising in multiscale models, the $t\bar{t}$ cross section is a very sensitive probe, and so the Tevatron has a mass reach for the $P_8^{0\prime}(\eta_T)$ of 400-500 GeV [80]. The color singlet technipions are more difficult to discover at a hadron collider than the color octet states since the latter can be strongly produced. In Run II, the reach for the color singlet technipion states will be 115 GeV. At LHC, older studies which do not take advantage of b tagging indicate that the color octet technipions are observable through direct production up to a mass of about 325 GeV and that the LHC will be able to see the charged color singlet technipions to a mass reach of about 400 GeV. The same studies indicate that the neutral singlet technipions will be accessible to 100–150 GeV at LHC [80].

B. Technirho ρ_T

We have discussed in detail the mass reach of the LHC and of a 1.5 TeV linear collider for the color singlet ρ_T. However, lower energy machines are also sensitive to its discovery. The linear collider operating at $\sqrt{s} = 500$ GeV can discover a ρ_T up to at least 1.5 TeV via the same helicity analysis of $e^+e^- \to W^+W^-$ that was described earlier (and, again, with the assumption that a single resonance dominates the form factor) [9]. In fact, by the same technique, LEP 2 can discover a ρ_T up to 350 GeV [29]. The Tevatron will have a discovery reach of approximately 200 GeV in run II and 400 GeV at TeV33. As was the case with technipions, the color octet technirho states are more easily accessible than the singlets at a hadron collider. The Tevatron currently excludes a color octet technirho up to 500 GeV and TeV33 will be sensitive to color octet ρ_T's up to a mass of about 900 GeV [79].

C. Topcolor B and Z'

In topcolor assisted technicolor, there is a top gluon (B) that couples mainly to top and bottom quarks and a massive color singlet gauge boson (Z'). The mass reach for topgluons is 1.0-1.1 TeV for the Tevatron in Run II and is 1.3-1.4 TeV for TeV33 [79]. The sensitivity to the Z' depends on the couplings of the Z' to the light quarks. In the optimistic case where the coupling is comparable to the couplings of the quarks to the Z, TeV33 will be sensitive to the Z' up to a mass of 1.1 TeV. The LHC should be sensitive over the entire range of expected masses for both the top gluon and topcolor Z' and will find them if they are there [79, 81].

Table VI: Mass reach in model-dependent searches for exotica discussed in Section IX. All mass limits are in TeV. The dashes represent cases for which we could not find results in the literature.

	NLC			Tevatron			LHC
	0.5	1.0	1.5	Run I	Run II	TeV33	
Technipion $P^{\pm}$	0.25	0.5	0.75	–	0.1	–	0.3 - 0.4
Technipion $P_8^{0\prime}$	–	0.7	–	0.4-0.5	–	–	–
Technirho (singlet)	1.5	3.0	4.0	–	0.2	0.4	1.6
Technirho (octet)	–	–	–	0.5	–	0.9	–
Topcolor B	–	0.8?	–	–	1.1	1.4	found
Topcolor Z'		found		–	0.9	1.1	found
Top Higgs	0.18	0.55	–	–	–	–	0.7

There are no published analyses on the reach of NLC to discover topgluons; the search is difficult because the topgluons couple directly only to quarks. Some preliminary work [82] indicates that the topgluon can be observed at the 1 TeV NLC up to about 800 GeV, not as a resonance but rather through interference effects in $e^+e^- \to b\bar{b}b\bar{b}$. This point needs further study. On the other hand, the topcolor Z' couples to leptons and thus gives effects similar to those of other new Z bosons. The NLC even at 500 GeV would be sensitive to the topcolor Z' up to 3 TeV, covering the complete range of expectations for its mass [83].

D. Light ETC Exotica

Heavy particles which are are bound states of techniquarks with light ETC bosons (τ^* and t^*) will behave much like excited quarks and leptons. For excited quarks, the reach of TeV33 is 1.1 TeV and that of LHC is 6.3 TeV. For NLC(0.5/1.0) the reach is 0.45/0.9 TeV [9, 79]. These limits can be used as an estimate of the expected reach for the t^* and, in the case of the NLC, for the τ^*.

E. Top Higgs Sector

The π_t will be pair-produced through Drell-Yan production, with the dominant decays into weak boson pairs. The h_t is produced in much the same processes as a standard model Higgs, although the width and the branching fractions may be very different. At the NLC, a lower limit to the discovery reach comes from considering the conventional Higgs reaction $e^+e^- \to Z^0h^0$ with 10% of the standard cross section; this gives a reach of 180 GeV at 0.5 TeV and about 550 GeV at 1.0 TeV [9]. The latter reach is well above the expected value of $2m_t$. (In addition, the h_t should be visible as a resonance at a $\gamma\gamma$ collider.) We can obtain a similar lower limit to the discovery reach at the LHC by comparing the rate for the process $gg \to h_t \to Z^0Z^0$ to that for the Standard Model Higgs; this gives a reach of about 700 GeV [84]. Neither of these estimates makes use of the dominant decay of the top Higgs to $t\bar{t}$. More detailed, model-dependent assessments of the top Higgs sector discovery limits need to be made for all colliders.

The model dependent reach limits for the various explicit models of discussed in Section VIII are summarized in Table VI.

X. CONCLUSION

In this report, we have described two approaches to the experimental study of a strong-coupling mechanism of electroweak symmetry breaking. In the first few sections, we took the conservative point of view that any model of strong-coupling electroweak symmetry breaking must result in pion-pion strong interactions that could be observed in high energy WW scattering. We summarized the available experimental studies that have explored the reach of future experiments to uncover and study these new pion interactions, and we evaluated both the ability of the experiments to discover the new strong interaction, as well as the reach of experiments to probe the structure of the new strong interactions. We then turned to the study of specific models and discussed the wide variety of signatures which characterize them. In general, the models predict new particles which decay to heavy flavors and exotic interactions of the third-generation fermions. Thus, even if there is no single signature which is characteristic of the broad class of models, it is clear what general experiments one must do to probe this physics.

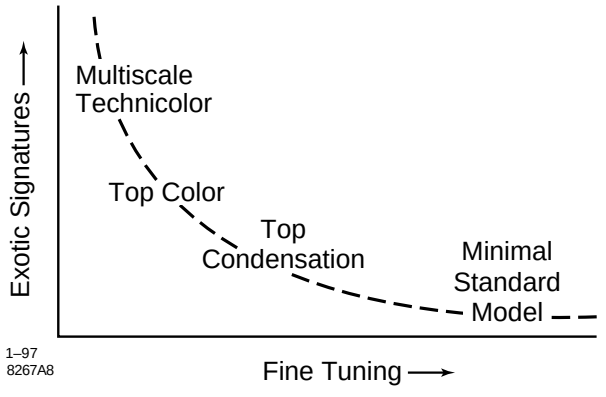

Figure 16: Diagram of strong-coupling model space, after Terning.

The tension between conservative, model-independent signa-

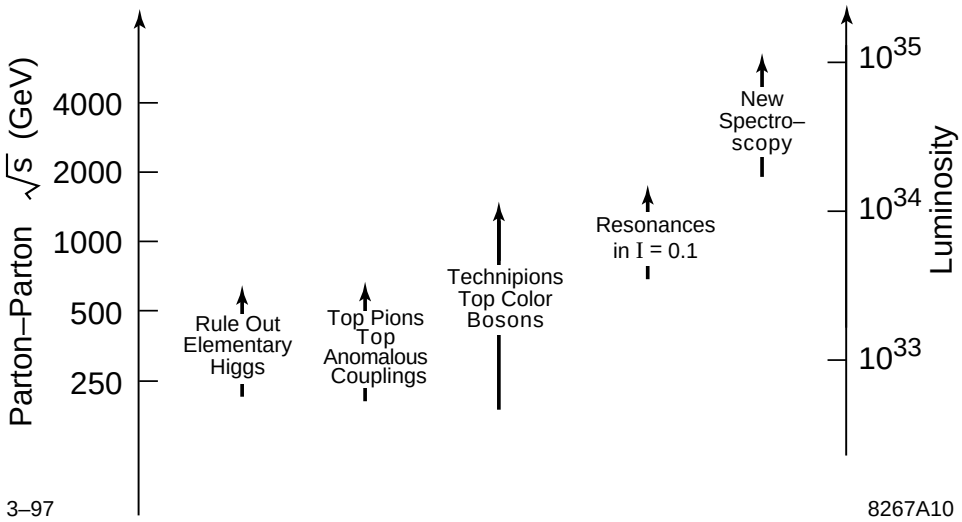

Figure 17: Program of experiments on strong-coupling electroweak symmetry breaking as a function of available energy and luminosity.

tures on one hand and exotic signatures on the other is illustrated in Figure 16. The axes in this figure are, vertically, the appearance of exotic signatures and, horizontally, the amount of fine-tuning implicit in the model. The scale is probably logarithmic in both cases. Models with a large number of wheels and gears naturally create a large number of exotic phenomena that one could try to observe at colliders. The further one goes in removing explicit dynamical mechanisms, the more one must rely experimentally on the most general, model-independent signatures. But also in this case, one must depend more and more on fine adjustments of the model to produce all of the physics which results from electroweak symmetry breaking.

In this report, we have listed a large number of model-dependent signatures of new strong interactions. The searches for these particles can begin at present accelerators and at the upgraded Tevatron. The demonstration that electroweak symmetry breaking comes from new strong interactions should also include the exclusion of a light Higgs boson coupling to WW and ZZ. In Figure 17, we indicate the experiments that will be important to the study of new strong interactions as the available energy and luminosity is increased.

However, the irreducible experimental question is that of the direct observation of new strong interactions in WW scattering processes. These experiments can be carried out at the LHC and can be confirmed and extended by a high-energy electron-positron collider. However, it will require pushing those machines to the limits of their design.

It is clear that should new strong interactions be discovered, we would then want to study their behavior at energies high compared to their natural scale. This study, which would be necessary to clarify the fundamental origin of the new interactions, would require accelerator facilities beyond the next generation—parton center-of-mass energies in excess of 5 TeV and luminosities in excess of 10^{35}. This study is not a realistic goal for currently feasible accelerators, and, even to imagine carrying out such an experimental program, it will be essential to first know that this is the path that Nature has chosen. For the near future, the crucial questions we must answer are simpler: Are there new strong interactions responsible for electroweak symmetry breaking? What is their general form? Where are their most important resonances? How does the top quark couple to these interactions, and why is the top quark so heavy? These are the questions that the working group focussed on. Our conclusions can be summarized as follows:

- The experiments are hard.
- We will need the highest energy and the full design luminosity of the proposed and upcoming colliders. Our conclusions assume the LHC at 14 TeV and the NLC at 1.5 TeV, in each case with 100 fb^{-1} data samples.
- The LHC can discover strong interaction electroweak symmetry breaking.
- The LHC can probe the effects of scalar resonances up to 1.6 TeV and vector resonances up to 1.6 TeV.
- The NLC at 1.5 TeV can probe the effects of resonances in the vector channel up to 4 TeV through an accurate measurement of the I=1 phase shift in $e^+e^- \to W^+W^-$.
- The NLC at 1.5 TeV can study the coupling of top to the symmetry breaking sector.
- Many, but not all, models of strong electro-weak symmetry breaking predict low energy phenomena in the mass range 200–700 GeV that can be searched for at the Tevatron, LHC, and NLC.

- A detailed understanding of strong electro-weak symmetry breaking will probably have to wait for machines with parton energies greater than 5 TeV and luminosities greater than 10^{35} cm^{-2}s^{-1}.

XI. REFERENCES

[1] W. Marciano, in these proceedings.

[2] M. Weinstein, Phys. Rev. **D8**, 2511 (1973).

[3] P. Sikivie, L. Susskind, M. Voloshin, and V. Zakharov, Nucl. Phys. **B173**, 189 (1980).

[4] M. E. Peskin and T. Takeuchi, Phys. Rev. Lett. **65**, 964 (1990), Phys. Rev. **D46**, 381 (1992).

[5] P. Langacker and J. Erler, hep-ph/9703428, and in Review of Particle Properties, Phys. Rev. **D54**, 1 (1996).

[6] H. E. Haber, T. Han, F. S. Merritt, and J. Womersley, in these proceedings.

[7] D. Amidei, *et al.*, Future Electroweak Physics at the Fermilab Tevatron, Fermilab-PUB-96/082 (1996).

[8] I. Hinchliffe and J. Womersley, eds., in these proceedings.

[9] S. Kuhlman, *et al.*, Physics and Technology of the Next Linear Collider, BNL 52-502, Fermilab-PUB-96/112, LBNL-PUB-5425, SLAC-Report-485, UCRL-ID-124160, UC-414 (1996).

[10] D. B. Kaplan and H. Georgi, Phys. Lett. **B136**, 183 (1984).

[11] A. E. Nelson and M. J. Strassler, hep-ph/9607362.

[12] J. M. Cornwall, D. N. Levin, and G. Tiktopoulos, Phys. Rev. **D10**, 1145 (1974);
C. E. Vayonakis, Lett. Nuov. Cim. **17**, 383 (1976).

[13] B. W. Lee, C. Quigg, and H. B. Thacker, Phys. Rev. Lett. **38**, 883 (1977), Phys. Rev. **D16**, 1519 (1977).

[14] M. S. Chanowitz and M. K. Gaillard, Nucl. Phys. **B261**, 379 (1985).

[15] M. S. Chanowitz and W. Kilgore, Phys. Lett. **B322**, 147 (1994).

[16] J. Bagger, V. Barger, K. Cheung, J. Gunion, T. Han, G. A. Ladinsky, R. Rosenfeld, and C. P. Yuan, Phys. Rev. **D49**, 1246 (1994), **D52**, 3878 (1995).

[17] J. Gasser and H. Leutwyler, Ann. Phys. **158**, 142 (1984), Nucl. Phys. **B250**, 465 (1985).

[18] S. Dawson and G. Valencia, Nucl. Phys. **B352**, 27 (1991).

[19] A. Dobado, M. J. Herrero, and J. Terron, Z. Phys. **C50**, 205, 465 (1991).

[20] J. R. Peláez, in these proceedings.

[21] W. Kilian, in these proceedings.

[22] CMS Collaboration, Technical Proposal, CERN report CERN/LHCC/94-38

[23] ATLAS Collaboration, Technical Proposal, CERN report CERN/LHCC/94-43.

[24] C.-E. Wulz, in Proceedings of the International Europhysics Conference on High Energy Physics, EPS HEP 95, J. Lemonne, C. Vander Velde, and F. Verbeure, eds. (World Scientific, Singapore, 1996).

[25] M. Golden, T. Han and G. Valencia, in Electroweak Symmetry Breaking and Beyond the Standard Model, T. Barklow, S. Dawson, H. Haber, and J. Siegrist, eds. (World Scientific, Singapore, 1996).

[26] D. Wood, in these proceedings.

[27] Barger, Cheung, Han and Phillips, Phys Rev **D52**, 3815 (1995).

[28] T. Barklow, in these proceedings.

[29] T. Barklow, in Physics and Experiments with Linear Colliders, A. Miyamoto, Y. Fujii, T. Matsui, and S. Iwata, eds. (World Scientific, Singapore, 1996).

[30] M. Chanowitz, M. A. Furman, and I Hinchliffe, Phys. Lett. **B78** 285 (1978), Nucl. Phys. **B153**, 402 (1979).

[31] T. Appelquist and M. S. Chanowitz, Phys. Rev. Lett. **59**, 2405 (1987), E **60**, 1589 (1988).

[32] M. Golden, Phys. Lett. **B338**, 295 (1994).

[33] R. P. Kauffman, Phys. Rev. **D41**, 3343 (1990);
M. Gintner and S. Godfrey, in these proceedings.

[34] W. Kilgore, in these proceedings.

[35] V. Barger, M. S. Berger, J. F. Gunion, and T. Han, Phys. Rev. **D55**, 142 (1995).

[36] M. Chanowitz and M. K. Gaillard, Phys. Lett. **B142**, 85 (1984).

[37] D. A. Morris, in Workshop on Current Accelerators and the Supercolliders, J. L. Hewett, A. R. White, and D. Zeppenfeld, eds. ANL-HEP-CP-93-92.

[38] T. Barklow, *et al.*, in these proceedings.

[39] J. Bagger, S. Dawson, and G. Valencia, Nucl. Phys. **B399**, 364 (1993).

[40] A. F. Falk, M. Luke, and E. H. Simmons, Nucl. Phys. **B365**, 523 (1991).

[41] H. Aihara, *et al.*, in Electroweak Symmetry Breaking and Beyond the Standard Model, T. Barklow, S. Dawson, H. Haber, and J. Siegrist, eds. (World Scientific, Singapore, 1996).

[42] K. Hagiwara, S. Ishihara, R. Szalapski, and D. Zeppenfeld, Phys. Lett. **B283**, 353 (1992).

[43] S. Weinberg, Phys. Rev. **D19**, 1277 (1979).

[44] L. Susskind, Phys. Rev. **D20**, 2619 (1979).

[45] E. Eichten and K. Lane, Phys. Lett. **B90**, 125 (1980).

[46] S. Dimopoulos and L. Susskind, Nucl. Phys. **B155**, 237 (1979).

[47] E. Eichten, K. Lane, and J. Preskill, Phys. Rev. Lett. **45**, 225 (1980).

[48] S. Dimopoulos and J. Ellis, Nucl. Phys. **B182**, 505 (1982).

[49] T. Appelquist, M. J. Bowick, E. Cohler, and A. I. Hauser, Phys. Rev. **D31**, 1676 (1985).

[50] T. Appelquist, M. Einhorn, T. Takeuchi, and L.C.R. Wijewardhana, Phys. Lett. **B220**, 223 (1989);
V.A. Miransky and K. Yamawaki, Mod. Phys. Lett. **A4**, 129 (1989);
K. Matumoto, Prog. Theor. Phys. Lett. **81**, 277 (1989).

[51] B. Holdom, Phys. Rev. **D24**, 1441 (1981).

[52] B. Holdom, Phys. Lett. **B150**, 301 (1985).

[53] K. Yamawaki, M. Bando, and K. Matumoto, Phys. Rev. Lett. **56**, 1335 (1986).

[54] T. Appelquist, D. Karabali, and L. C. R. Wijewardhana, Phys. Rev. Lett. **57**, 957 (1986);
T. Appelquist, and L. C. R. Wijewardhana, Phys. Rev. **D35**, 774, **D36**, 568 (1987).

[55] N. Seiberg, Nucl. Phys. **B435**, 129 (1995).

[56] T. Appelquist, J. Terning, and L.C.R. Wijewardhana, Phys. Rev. Lett. **77**, 1214 (1996).

[57] M. E. Peskin, Nucl. Phys. **B175**, 197 (1980);
J. P. Preskill, Nucl. Phys. **B177**, 21 (1981).

[58] K. Lane and E. Eichten, Phys. Lett. **B222**, 274 (1989).

[59] K. Lane and M. V. Ramana, Phys. Rev. **D44**, 2678 (1991).

[60] K. Lane and E. Eichten, Phys. Lett. **B327**, 129 (1994).

[61] K. Lane, in The Building Blocks of Creation (TASI-93), S. Raby and T. Walker, eds. (World Scientific, Singapore, 1994).

[62] T. Appelquist, M. Einhorn, T. Takeuchi, and L. C. R. Wijewardhana, Phys. Lett **B220**, 223 (1989);
V. A. Miransky and K. Yamawaki, Mod. Phys. Lett. **A4**, 129 (1989);
K. Matumoto, Prog. Theor. Phys. Lett. **81**, 277 (1989);
R. S. Chivukula, K. Lane, and A. G. Cohen, Nucl. Phys. **B343**, 554 (1990);
T. Appelquist, J. Terning, and L. C. R. Wijewardhana, Phys. Rev. **D44**, 871 (1991).

[63] R.S. Chivukula, E. Gates, E.H. Simmons, and J. Terning, Phys. Lett. **B311** 157 (1993).

[64] R. S. Chivukula, Phys. Rev. Lett. **61**, 2657 (1988);
B. Holdom, Phys. Lett. **B226**, 137 (1989);
T. Appelquist, M. Einhorn, T. Takeuchi, and L. C. R. Wijewardhana, Phys. Lett **B220**, 223 (1989).

[65] R. S. Chivukula, S. B. Selipsky, and E. H. Simmons, Phys. Rev. Lett. **69**, 575 (1992).

[66] N. Kitazawa, Phys. Lett. **B313**, 395 (1993); K. Hagiwara and N. Kitazawa, Phys. Rev. **D52**, 5374 (1995).

[67] Guo-Hong Wu, Phys. Rev. Lett. **74** (1995) 4137.

[68] R. S. Chivukula, E. Gates, E. H. Simmons and J. Terning, Phys. Lett **B311**, 157 (1993);
R. S. Chivukula, E. H. Simmons and J. Terning, Phys. Lett **B331**, 383 (1994).

[69] H. Murayama, in Physics and Experiments with Linear Colliders, A. Miyamoto, Y. Fujii, T. Matsui, and S. Iwata, eds. (World Scientific, Singapore, 1996).

[70] U. Mahanta, hep-ph/9607227.

[71] P. Arnold and C. Wendt, Phys. Rev. **D33**, 1873 (1986).

[72] T. Appelquist and N. Evans, Phys. Rev. **D53**, 2789 (1996).

[73] C. T. Hill, Phys. Lett. **B266** (1991) 419.

[74] C. T. Hill, Phys. Lett. **B345**, 483 (1995).

[75] R. S. Chivukula, A. G. Cohen, and K. Lane, Nucl. Phys. **B343**, 554 (1990);
T. Appelquist, J. Terning, and L.C.R. Wijewardhana, *Phys. Rev.* **D44**, 871 (1991).

[76] G. Burdman, in these proceedings.

[77] OPAL Collaboration, Phys. Lett. **B242**, 299 (1990).

[78] M. Swartz, in these proceedings.

[79] K. Cheung and R. M. Harris, in these proceedings.

[80] R. S. Chivukula, R. Rosenfeld, E. H. Simmons, and J. Terning, in Electroweak Symmetry Breaking and Beyond the Standard Model, T. Barklow, S. Dawson, H. Haber, and J. Siegrist, eds. (World Scientific, Singapore, 1996).

[81] R. M. Harris, in these proceedings.

[82] E. Sather, private communication.

[83] S. Godfrey, J. L. Hewett, and L. E. Price, in these proceedings.

[84] J. Wells, private communication.